IEEE Access
Multidisciplinary ⋮ Rapid Review ⋮ Open Access Journal

Received 23 February 2023, accepted 18 March 2023, date of publication 24 March 2023, date of current version 29 March 2023.
Digital Object Identifier 10.1109/ACCESS.2023.3261547

TOPICAL REVIEW

Review Paper on Hardware of Reconfigurable Intelligent Surfaces

BISWARUP RANA [1], SUNG-SIL CHO [2], AND IC-PYO HONG [2], (Member, IEEE)
[1]Smart Natural Space Research Centre, Kongju National University, Cheonan 31080, South Korea
[2]Department of Smart Information Technology Engineering, Kongju National University, Cheonan 31080, South Korea
Corresponding author: Ic-Pyo Hong (iphong@kongju.ac.kr)

This work was supported by the Underground City of the Future Program funded by the Ministry of Science and ICT.

ABSTRACT Recently reconfigurable intelligent surface (RIS) has attracted great attention because it can create a smart wireless environment. Hence it can enhance the capacity and coverage of the wireless network significantly. A thorough review of RISs has been presented in this paper focusing on the hardware aspect of the RIS. Beyond-5G/6G communication will have a smart propagation environment, where RIS can be used for such communications. RIS consists of various small unit cells. The unit cells should have some tunning mechanism to reflect or transmit the incoming waves in the desired direction. It is possible to tune the impedance of the unit cells using PIN diodes, varactor didoes, microelectromechanical (MEMS), thermal, and other ways. In this paper, the background of RIS has been discussed where RIS will play a significant role in beyond-5G/6G communications. We have also added the theoretical background of RIS and motivations to writing this paper. After that several published papers in the literature have been presented so that the readers can get an overall idea about the RIS and its hardware. Hence, this paper will be very useful for practitioner engineers and researchers. RISs have been presented in various tables and various parameters have been presented. We have discussed challenges and solutions for the hardware of the RIS design. We have also discussed potential research and research gap that can be explored in the future. Lastly, we have added a conclusion for this review paper. In our manuscript, we have added 154 references. There are various kinds of RIS available in the literature. We have added different types of RISs in this manuscript. The magnitude and phase of the reflection and transmission coefficients are the main parameters of any kind of RIS.

INDEX TERMS Reconfigurable intelligent surface (RIS), beyond-5G/6G communication, reflectarray, PIN diode, varactor diode.

I. INTRODUCTION

With the introduction of the ''Intelligent Wall'' concept for the smart indoor environment, researchers and engineers worldwide are being focused on creating smart wireless environments for signal propagation [1]. While the 5G technology is being deployed worldwide and various hardware for 5G technology is being developed, researchers across the globe are looking forward to the technology for beyond-5G/6G [2], [3], [4], [5], [6], [7], [8], [9], [10]. To meet the users' demands, first-generation to fifth-generation wireless technologies were conceived and designed. The design guidelines for the 5G communications were based on the initial three properties (a) enhanced mobile broadband (eMBB), (b) ultra-reliable and low latency communications (URLLC), (c) and massive machine type communications (mMTC) [11], [12], [13]. Beyond-5G/6G networks shall integrate ground, space, air, and underwater and perform better than the 5G networks. Beyond-5G/6G network will support several applications and services like brain-machine interface [14], [15], augmented reality [16], [17], virtual reality [18], [19], mixed reality, connected autonomous vehicles [20], [21], [22], connected robotics, connected unmanned aerial vehicles [23], [24], [25], [26], connected health [27], [28] smart cities [29], [30], indoor localization [31], [32]. Beyond-5G/6G network will have the following features:(a) Very low latency (approximately 10 μs) [33], (b) Tb/s peak data rate and end-to-end reliability requirement is 99.99999 percent [34], (c) Higher

The associate editor coordinating the review of this manuscript and approving it for publication was Mohammad Zia Ur Rahman.

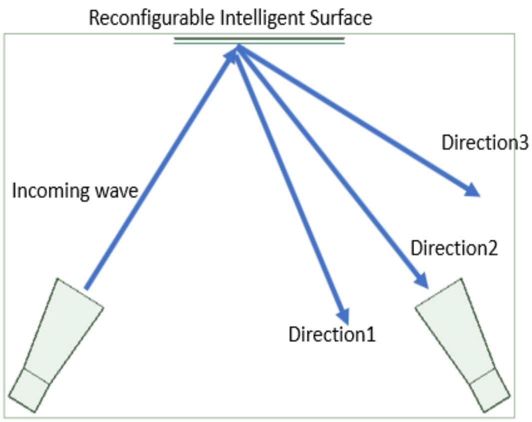

FIGURE 1. Reflective type reconfigurable intelligent surface.

energy and spectral efficiency compared to the 5G network, (d) Wide frequency range (like sub-6 GHz, mmWave, THz band, optical frequency, VLF, etc.), (e) Use of artificial intelligence and machine learning algorithms in the networks [35], (f) Intelligent transmitter and intelligent receiver with RISs. It is predicted that beyond-5G/6G communication will have a paradigm shift in communication systems like previous communication systems [36]. In [37], [38], [39], and [40] review of the RISs was presented describing its distinct feature, benefits of the RIS, and potential future use case of the RIS. Theoretical studies of RIS like beam-forming optimization were presented by various authors over the years [41], [42], [43], [44], [45], [46], [47]. In [48], the authors studied electromagnetic wave control using RIS as a near-field and far-field problem. Machine learning and artificial intelligence are being used in various applications. In [49] and [50], the authors used deep reinforcement learning or deep learning to optimize the RIS. The secrecy performance of an intelligent reflecting surface (IRS)-aided indoor wireless communication was investigated in [51]. In [52], the authors presented two computationally energy efficiency maximization algorithms for wireless communications. It is envisioned that the RIS will have a profound effect on beyond-5G/6G communications [53], [54], [55], [56], [57], [58], [59], [60], [61], [62], [63]. The literature has different names for RIS like intelligent reflecting surface [64], [65], [66], [67], [68], [69], [70], [71], [72], and large intelligent surface [73]. RIS allows the incoming waves to reflect in the desired directions. This property is very important because it can create a smart radio environment, increase the signal-to-noise ratio, increase energy efficiency, etc. Generally, phased array antennas are used to send the beam in the desired direction [74], [75], [76], [77], [78]. However, the phased array antenna is expensive and it needs lots of power to operate. A large number of phased array antennas can be used in beyond-5G/6G communications. However, it is not an efficient way to improve the performance of the network. RIS is an almost passive type structure allowing incoming waves to reflect/transmit in the desired direction. Hence, RIS can be very useful for beyond-5G/6G communications instead of a large number of phased array antennas. Also, RIS can be used as a transmitter or receiver instead of conventional base station antennas. RISs can not only be used in the beamforming scenario but also it can be used rich scattering environments [79], [80], [81]. It is expected that RIS can provide wideband connectivity in highly congested areas and indoor settings. Reconfigurable reflect arrays have been known and studied for a very long time. RIS and a reconfigurable reflect array are the same thing that can reflect the beam in the desired direction [82], [83], [84], [85], [86], [87]. The RIS also can be used as a transmissive mode. Normally the source antenna of the RIS is placed very far from the surface. However, the source can be placed near-field regions [88]. Fig. 1 shows the RIS in the reflective mode. As shown in Fig. 1, the beam can be reflected in different directions. A general controller can be used to change the impedance of the different unit cells. The controller can be a field programmable gate array (FPGA) or microcontroller or any other type of controller [89]. Transmissive type RIS will be also very useful for beyond-5G/6G communications. However, there is no significant research on the transmissive type RIS. The present authors envisioned that transmissive-type RIS will have a major impact on different types of communications in the future.

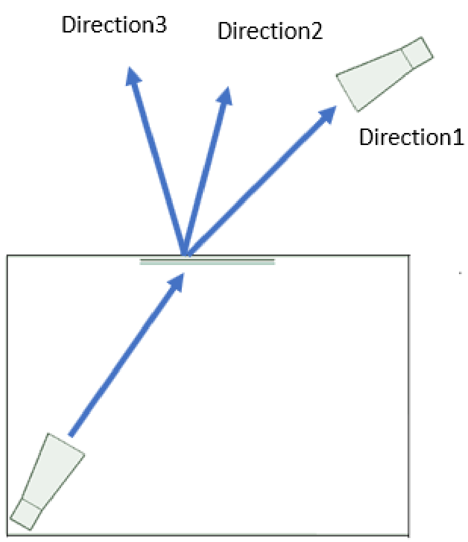

FIGURE 2. Transmissive type reconfigurable intelligent surface.

Fig. 2 shows the transmissive type of RIS. The incoming signal can be steered in different directions as shown in Fig. 2. The conventional base station for beyond-5G/6G can also be a RIS-enabled base station. Massive multi-input multi-output (MIMO) is being considered for 5G communications [90], [91]. Instead of a conventional massive MIMO antenna, reflective or transmissive type RIS can be very promising for beyond-5G/6G applications. The reflected wave or transmitted type waves can go depending upon the material properties and configuration of the unit cells. Normally, microstrip patches, metamaterial structures, or frequency selective surfaces are used to design the unit cell. The RIS can be fabricated using Printed Circuit Board (PCB) technology. PCB technology is very cost-effective to fabricate the unit cell and whole structures. Transmissive RIS is similar to reconfigurable transmitarray [92], [93], [94], [95], [96], [97], [98], [99], [100], [101], [102] while reflective RIS is similar to reconfigurable reflectarray [103], [104], [105]. Both RIS and reconfigurable reflectarray/reconfigurable transmitarray use spatial feeding techniques. A horn antenna, an antenna array, or other types of sources are being used to feed such type structures. In the literature, there are several review papers on RIS and related review papers. In [37], the authors presented an introduction to IRS and its reconfigurability. Then the authors discussed applications of the IRS in wireless communications. Different performance metrics and analytical approaches of the IRS were presented in that paper. In [38], the authors presented a review of RIS, its current limitations, and the future development of RIS. An emerging area of RIS-empowered smart radio was discussed in [40]. The authors discussed applications of the RISs in wireless communications and presented an electromagnetic-based communication-theoretic. In [56], the authors discussed the working principle of the RIS and presented channel modeling for such environments. In [59], the authors presented the theoretical performance limits of the RIS-assisted communications system. In [64], an overview of the RIS was discussed including its applications in the wireless channel, the benefit of the RIS over other technology, the hardware of the RIS, and the signal model. The authors discussed the theoretical basis of the metasurface and its various applications [106]. The uniqueness of the metasurface was compared to the frequency-selective surface. In [107] an overview of the smart radio environment was presented. The paper also discussed the long-term and open research issues to be solved for mass deployment. An overview of RIS was presented in [108]. The authors discussed the reflection properties of the RIS, its channel model, hardware architecture, and practical limitations of the RIS. The authors also gave future research directions for RIS. An overview of the large intelligent surface/antenna (LISA) was presented in [109]. The authors also discussed the limitations, challenges, and open issues of the LISA. In [110], a detailed review of the RIS was presented. Also, there are other several review papers on RIS available in the literature. However, none of those papers gives details of the hardware aspect of the RIS. In this paper, we have reviewed many RIS that will be useful for scientists or researchers whose main aim is to design IRS hardware. Table 1 shows a comparison of various review papers on RIS [37], [38], [40], [56], [59], [64], [106], [107], [108], [109], [110]. In this manuscript, we have reviewed extensively the hardware of RISs. The following are the contributions of this review paper: 1) Various review papers on the RIS available in the literature are presented and tabulated. The uniqueness of our review paper is presented. Our paper focuses on the hardware aspect of the RIS. Thus, this paper will be useful to get an idea about the hardware of the RIS and it can be useful to design future hardware of RIS. 2) Some theories and formulas based on the surface impedance of the RIS are discussed which will be useful for the hardware of RIS designers. Also, we tabulate various other papers discussing the operating principles of RIS. So, readers of this paper get the theoretical background of RIS. 3) A large number of RIS available in the literature is discussed. From this literature review, engineers and scientists can get an overall idea of the hardware of RIS and they can design RIS according to their needs for various scenarios. 4) Challenges and solutions for the hardware of the RIS are discussed. The most important thing in the hardware design is cost-effective hardware with good performance. 5) Potential research and research gaps that can be explored in the hardware of the RIS design are presented. In this manuscript, different types of RIS available in the literature have been discussed. Initially, the operating principle of RIS has been presented in Section II. After that, different types of RIS available in the literature have been discussed in Section III. Various comparison tables have been presented highlighting features of different types of RIS in Section III. We have presented switching elements and materials in Section IV. In Section V, challenges and solutions to design RIS have been presented. We have discussed potential research gaps and research that could be explored in Section VI. In Section VII, conclusions have been presented.

TABLE 1. Review papers on RIS.

Ref.	Year	Contributions
106	2012	Discussed theories of the metasurface and its various applications
107	2019	Overview of the current research on the smart radio environment
109	2019	Discussed basics of large intelligent surface/antennas (LISA) including backscatter communications, reflective relay, and implementation of the LISA in actual scenario.
59	2019	Presented theoretical performance limit of the RIS-assisted communications system using mathematical techniques, disused the use case of the RIS for 6G and beyond wireless networks
64	2020	Provided an overview of the IRS, discussed advantages of the RIS, challenges to designing IRS
37	2020	Presented literature review on recent applications and design aspects of RIS
56	2020	Presented working principle of the RIS, discussed channel modeling
40	2020	Introduced RIS-empowered smart radio environments, presented applications of the RIS in wireless comminutions
108	2021	Provided a tutorial on RIS, reflection, channel models, hardware architecture, and practical limitations were discussed.
38	2022	Presented review on IRS, discussed limitations in the current research, discussed RIS-related research opportunity
110	2022	The recent progress of RIS was discussed.
Our Work	2023	We have presented an overview of the RIS emphasizing hardware. This review paper will be useful for engineers and researchers for actual fabrications of the RIS.

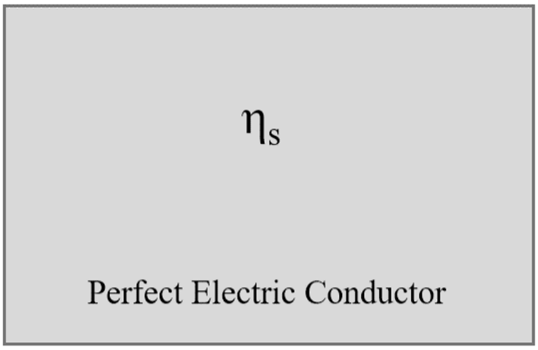

FIGURE 3. Perfect electric conductor with the same surface impedance.

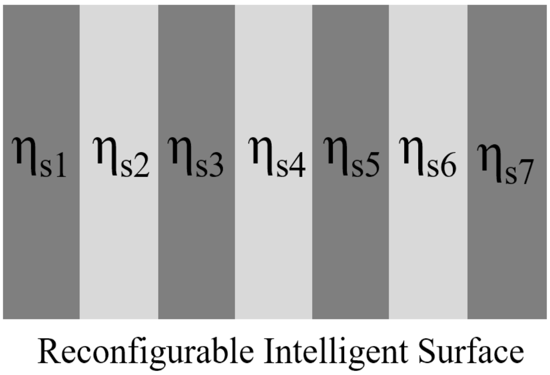

FIGURE 4. Reconfigurable intelligent surface with different surface impedances.

II. OPERATING PRINCIPLE OF RIS

RIS can be designed using metamaterial-based unit cells or patch types of unit cells or other types of techniques. The reflected waves or transmitted waves from the RIS can be reconfigured. The incident wave on the RIS can also be refractive. The imping wave on the RIS surfaces can be studied using Love's field equivalence principle [39], [111]. Also, the reflected waves can be represented using an equivalent electric current or magnetic current [112]. Huygens-Fresnel principle is also useful to calculate the field strength at any arbitrary point. Huygens-Fresnel principle states that every point on a wavefront is itself the source of spherical wavelets, and the secondary wavelets emanating from different points mutually interfere. In [113] physics-based end-to-end model of RIS-parametrized wireless channels with adjustable fading is presented. That was conceived from the first principles of coupled-dipole formalism. An end-to-end mutual coupling aware RIS model was presented in [114]. RISs are composed of a very large number of unit cells. Each unit cell can be tuned to have a different impedance. Fig. 3 shows a perfect electric conductor which has the same impedance on the surface namely η_s. So, the angle of reflected waves and the angle of incoming angle is the same for the perfect electric conductor.

However, for the RIS, the impedance of the surface can be varied from one point to another point on the surface as shown in Fig. 4. η_{s1}, η_{s2}, η_{s3}, η_{s4}, η_{s5}, η_{s6}, and η_{s7} are the different impedances of the surfaces in Fig. 4. The variation of the impedances on the surfaces causes phase changes of the reflected waves. The phase can be varied dynamically by varying the impedance of the surface continuously at a given area of the RIS. Hence, by varying the impedance of the surface of the RIS, constructive interference occurs in the desired direction. Again, by changing the impedance of the surface of the RIS, constructive interference occurs in different directions. Hence, a RIS can be obtained by varying the impedance of the surface. The surface impedance of the surface is related to the reflection coefficient of the surface and the reflection coefficient is expressed as [115]

$$\Gamma = (\eta_s - \eta_0)/(\eta_s + \eta_0) \quad (1)$$

where Γ is the reflection coefficient, η_s is the surface impedance, and η_0 is the free space wave impedance. The transmission coefficient can be expressed as

$$1 + \Gamma = (2\eta_s)/(\eta_s + \eta_0) \quad (2)$$

Equation (1) and Equation (2) are valid in an area where the surface impedance is the same. The reflection coefficients of the RIS for different areas can be expressed as

$$\Gamma_n = (\eta_{sn} - \eta_0)/(\eta_{sn} + \eta_0) \quad (3)$$

where n=1,2,3,4,5,6, and 7. η_0 is the free space wave impedance. $\eta_{sn}$is the impedance of the surface for different regions of the surface. So, the reflection coefficients are different for different areas of the RIS. Table 2 summarizes the operating principles of the RIS available in the literature with our explanations of the operating principle of the RIS [39], [111], [112], [113], [114].

TABLE 2. Summarization of operating principles.

Ref.	Contributions
39, 111	Discussed Love's field equivalence principle applicable to RIS
112	Discussed reflected waves and their equivalent electric and magnetic currents
113	End-to-end model of RIS-parametrized wireless channels with adjustable fading
114	An end-to-end mutual coupling aware RIS model
Our	Use surface impedance to explain the operating principle of the RIS

III. STATE-OF-THE-ART ON RECONFIGURABLE INTELLIGENT SURFACES

RIS is a very new area of study. It is expected that RIS will contribute significantly to beyond-5G/6G communications which will be deployed around 2030. In the literature, most papers are focusing on the theoretical aspect of RIS. However, designing a RIS and fabricating the hardware for RISs are very limited till now. In the literature, maximum papers are focusing on reflective type RIS, there are very limited transmissive type RIS. The present authors envisioned that both transmissive type and reflective types RIS shall play a significant role in beyond-5G/6G communication. There are different types of mechanisms through which the RIS can be fabricated like 1-bit with a PIN diode, 2-bit with a PIN diode, varactor diode based, etc. Some of the published papers are discussed in this section. This section is subdivided into several subsections. We have added earlier RIS in subsection A. B subsection discusses varactor didoes-based RISs available in the literature. PIN diode-based RISs are presented in subsection C. In the future, transmissive type RIS is going to play a crucial role. In subsection D, a transmissive type of RIS is presented. RIS-based wireless power transfer is discussed in subsection E. In subsection F, 3D graphene meta-atom-based RIS is discussed. 2.75-bit, 3-bit, and multi-bit RISs are presented in subsection G. In subsection H, multi-functional RIS is discussed. We have discussed RF-switch-based RIS in subsection I. Amplifying RIS is a very promising RIS. In subsection J, amplifying type of RIS is presented. Vanadium dioxide can be used as a tunable material to design RIS and VO_2-based RIS is presented in subsection K. Not only beam-forming of the RIS but also rich scattering from the RIS will be useful for indoor environments. We have added some literature reviews on RIS with a rich scattering in subsection L. RIS with on-chip is discussed in subsection M. In the N subsection, we have discussed passive types of RIS working at 3.5 GHz. Liquid crystal-based RISs are discussed in subsection O.

A. EARLY RECONFIGURABLE INTELLIGENT SURFACES

In [116], the authors derived generalized sheet transition conditions for the average electromagnetic fields across a metafilm. They calculated the reflection and transmission coefficients of the metafilms. By controlling the polarization densities of the scatters in the metafilm a ''smart'' and/or ''controllable'' surface was realized. Spherical magneto-dielectric particles were used to achieve a controllable surface and Fig. 5 shows such magneto-dielectric spherical particles. The structure had a radius of 0.41 cm and the space between center to center was 1.1 cm. In [117], the authors proposed a large electronically reconfigurable reflectarray which consists of a 160 × 160 reflecting surface. Microstrip patches and PIN diodes were used to construct such electronically reconfigurable reflectarray.

Fig. 6 shows the fabricated reflectarray working at the 60 GHz frequency band. In [118], ''digital metamaterial'' was proposed. Initially, the authors proposed ''coding metamaterial'' consists of two-unit cells with 0 and π phase response. Different functionalities can be achieved by a controlled sequence of 0 and π phases. Finally, the authors realized ''programable metamaterial''. Fig. 7 shows the flow diagram for realizing a programmable metasurface. In [119], the authors proposed a binary state tunable phase reflector based on the hybridized resonator. This concept can be applied at any other frequency and also this method is robust fluctuations induced by a tunable mechanism. Fig. 8 shows the experimental cell where the PIN diode was added.

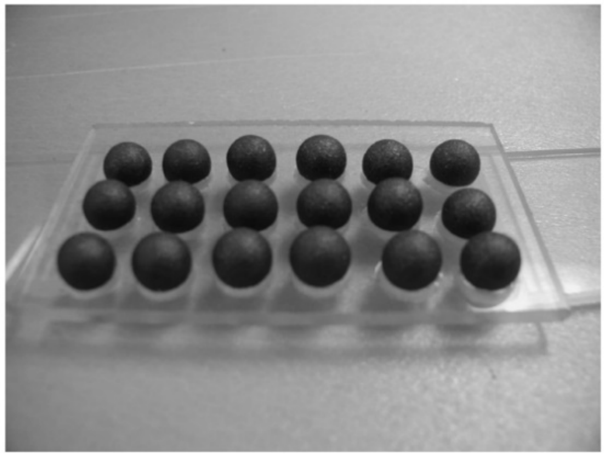

FIGURE 5. Magneto-dielectric spherical particles-based metafilms (images extracted from the work presented in [116]).

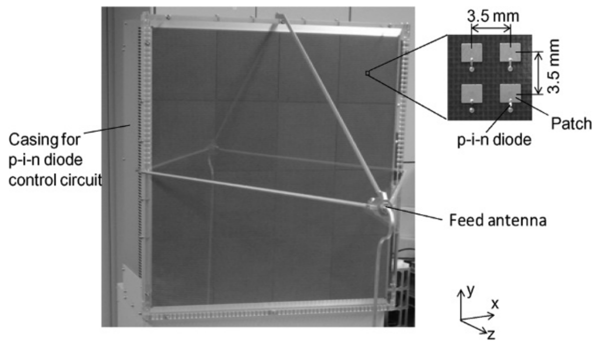

FIGURE 6. Fabricated reflectarray antenna (images extracted from the work presented in [117]).

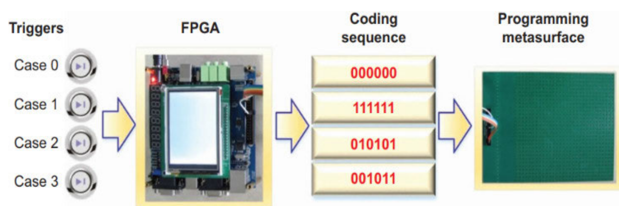

FIGURE 7. A flow diagram for realizing a programable metasurface (images extracted from the work presented in [118]).

In [1], the author introduced an intelligent wall based on an active frequency selective surface for the cognitive wireless network. The authors used an artificial neural network to learn the configurable environment. The concept of the intelligent wall was illustrated and the performance was evaluated based on the simple implementation of the arrangement of two intelligent walls in a conference center scenario.

B. VARACTOR DIODE-BASED RIS

Varactor didoes are some special diodes that can provide variable capacitance with changing voltage. The capacitance

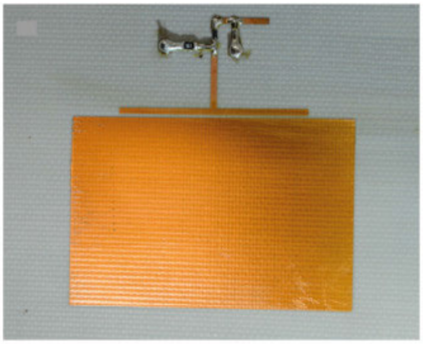

FIGURE 8. Fabricated cell (images extracted from the work presented in [119]).

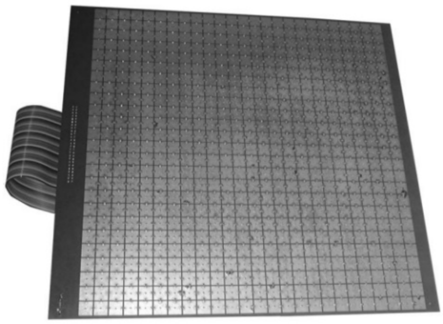

FIGURE 9. Photograph of the electronically steerable reflector (images extracted from the work presented in [121]).

of the varactor diode can be expressed as [120]

$$C(V) = K/(\varphi + V)^{n} \quad (4)$$

where C=dQ/dV and it is incremental diode capacitance, φ is the built-in potential, K is a constant, V is the total voltage, and n is the power law exponent. If the capacitance of the unit cell can be changed, the impedance will change and consequently, the reflected waves can be manipulated using a varactor diode. In [121], the authors used a metal ground plane with a periodic surface texture to alter its electromagnetic properties. By adding varactor diodes into the texture, a tunable impedance surface was conceived where the bias voltage controls the resonant frequency and the reflection phase. The surface could be tuned to get a phase gradient that was able to give a +/- 40° steered reflected beam. Fig. 9 shows the proposed electronically steerable reflector where 1125 varactors were added.

In [122], the authors proposed a varactor diode-based RIS operating in the sub-6 GHz frequency band. The frequency of operation of the proposed design was 3.5 GHz. The structure was composed of 2430-unit cells. A varactor diode was used to reconfigure the reflected beam. An equivalent circuit model was presented to verify the unit cell performance. Six PCB boards were fabricated. After that those six borders were merged to get a big PCB with dimensions of 120 mm×120 mm. A control unit with a custom-built

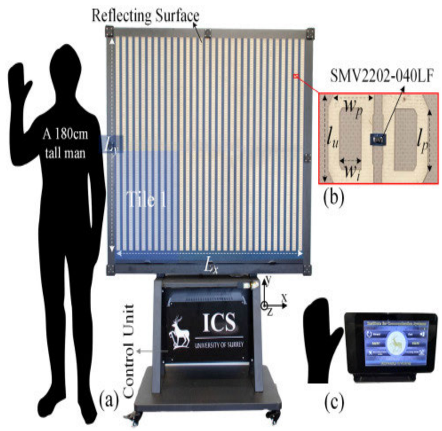

FIGURE 10. (a) RIS prototype with a control unit (b) the proposed unit cell (c) the portable controller (images extracted from the work presented in [122]).

system was also presented in the paper. Fig. 10(a) shows the fabricated prototype RIS while Fig. 10(b) and Fig. 10(c) show the unit cell and control board of the RIS, respectively. The functionality of the RIS in an indoor real-world environment was tested. Fig. 11 shows the unit cell response for 0.5-2 pF capacitance values of the capacitor at 3.5 GHz. It can be observed from Fig. 11 that by varying the capacitance of the capacitor, the required phase variation was obtained with low reflection loss.

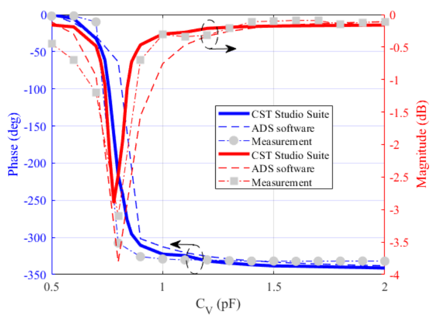

FIGURE 11. Response of the unit cell versus different capacitance values of the varactor diode at 3.5 GHz (images extracted from the work presented in [122]).

In [123], another varactor diode-based RIS was proposed. The authors used 1100 controllable elements working at 5.8 GHz. An efficient algorithm was proposed in that paper for configuring the RIS over the air. In the short-distance measurement environment, a power gain of 27dB was observed. The authors also measured the performance of the RIS in the outdoor long-distance scenario over 500 m. Very satisfactory performance of the RIS was observed in the outdoor measurement scenario also. Fig. 12 (a), Fig. 12 (b), and Fig. 12 (c) show the perspective view, top view, and side view of the proposed unit cell. The authors fabricated the design and measured its performance. Fig. 13 shows the fabricated 55 × 20 RIS. The authors varied the biasing voltage of the varactor diode from 0 V to 19 V to get at least 180° phase variation. Fig. 14 shows the magnitude and phase variation of the proposed design under different biasing voltages.

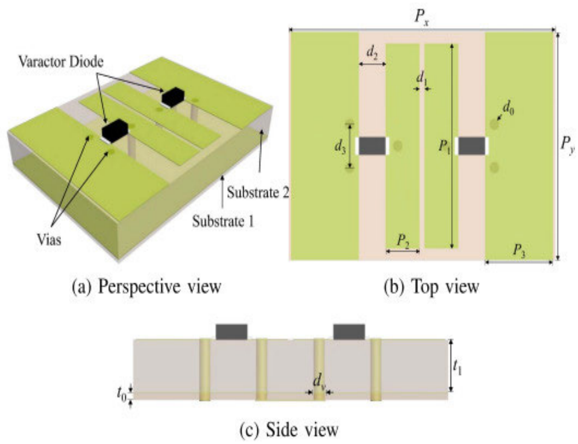

FIGURE 12. (a) Perspective view (b) top view (c) side view of the proposed unit cell (images extracted from the work presented in [123]).

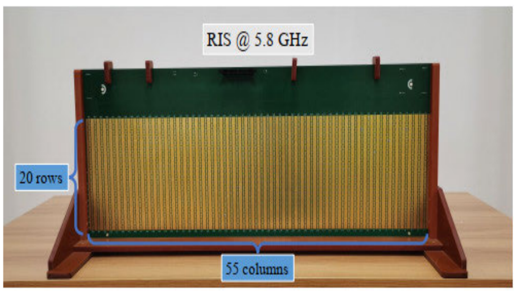

FIGURE 13. The front view of the fabricated 55 × 20 RIS (images extracted from the work presented in [123]).

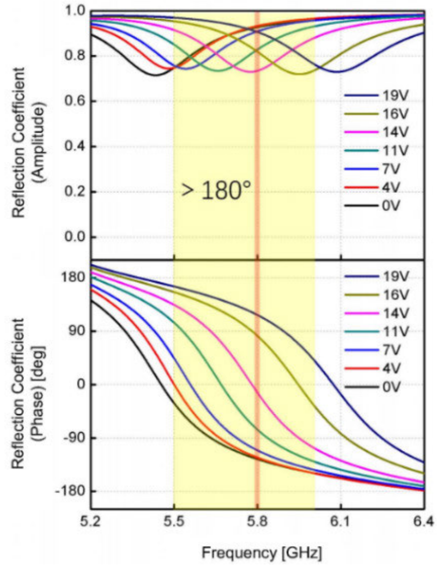

FIGURE 14. The simulated reflection amplitude and phase response of the RIS element under different voltages from 0 to 19 V (images extracted from the work presented in [123]).

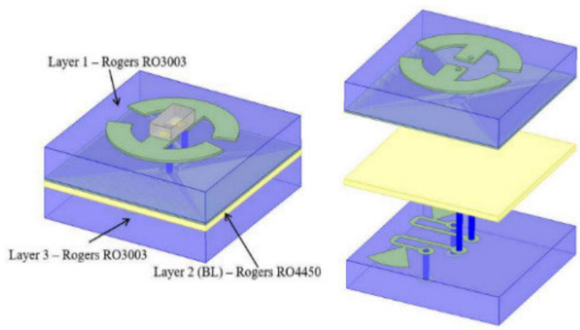

FIGURE 15. Unit cell and a bias circuit (images extracted from the work presented in [124]).

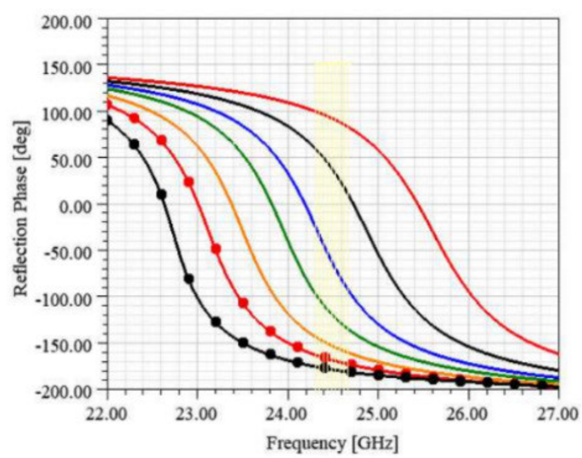

FIGURE 16. Reflection phase (images extracted from the work presented in [124]).

In [124], the authors proposed a varactor diode-based unit cell of the RIS as shown in Fig. 15. Varactor diode with a split-ring was considered to design the proposed unit cell. A phase shift of 277° as shown in Fig. 16 at 24.5 GHz with a minimum reflection amplitude of 0.5 was achieved with the proposed unit cell. In [125], a varactor diode-based RIS was proposed as shown in Fig. 17. The proposed RIS improved the system performance significantly and the model was optimized for the RIS-assisted AmBC system.

Table 3 compares the latest development of the Varactor diode-based RIS [121], [122], [123], [124], [125]. It has been noticed from the table that nowadays maximum authors are focusing to design in the sub-6 GHz frequency band.

C. PIN DIODE-BASED RIS

A 2-bit low-cost high-gain RIS was proposed in [126]. The proposed structure with modular hardware and fixable software had 256 elements. At 2.3 GHz, the proposed structure showed a gain of 21.7 dBi and at 28.5 GHz the gain was 19.1 dBi.

Fig. 18(a) and Fig. 18(b) show the exploded view and detailed view of the proposed 2-bit unit cell containing a

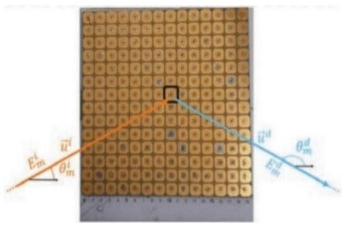

FIGURE 17. The fabricated RIS (images extracted from the work presented in [125]).

TABLE 3. Comparison of varactor diode-based RIS.

Ref.	Unit cell type	Control mechanism	Freq.	Remarks
121	Metal plate with vias	Varactor diode	4.5 GHz	Tunable impedance surface, steer reflected beam over + 40 in two dimensions
122	D-shaped patch	Varactor diode	3.5 GHz	2430-unit cells
123	Patch	Varactor diode	5.8 GHZ	1100 controllable elements
124	Split-ring	Varactor diode	24.5 GHz	Only simulated results
125	Conductive patch separated by the annular slot	Varactor diode	5.15 - 5.75 GHz	Continuous phase control

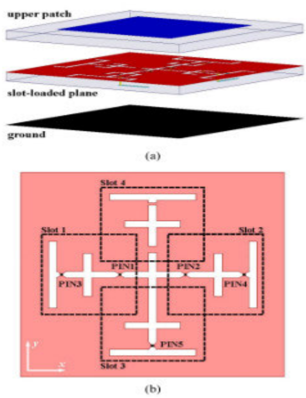

FIGURE 18. Proposed 2-bit unit cell: (a) exploded view; (b) detailed view of the slot-loaded plane (images extracted from the work presented in [126]).

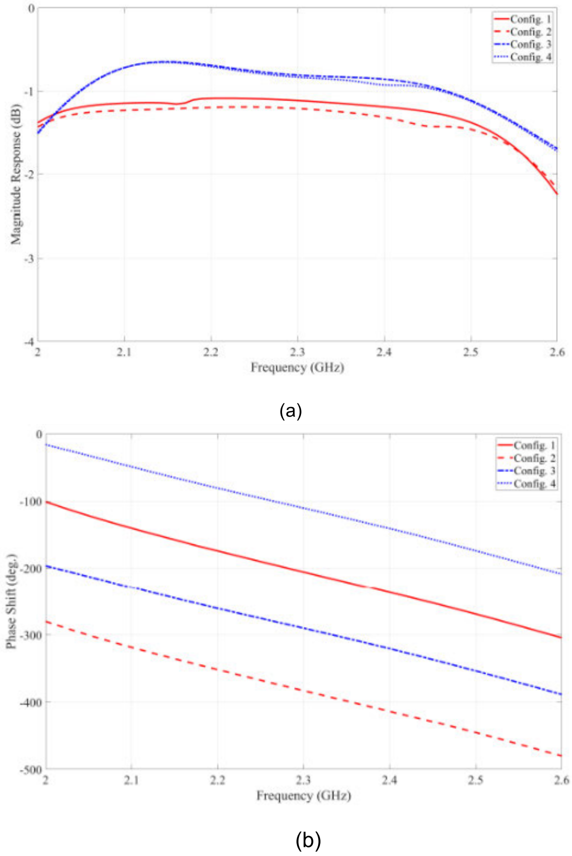

FIGURE 19. (a) Simulated magnitude (b) phase of the unit cell (images extracted from the work presented in [126]).

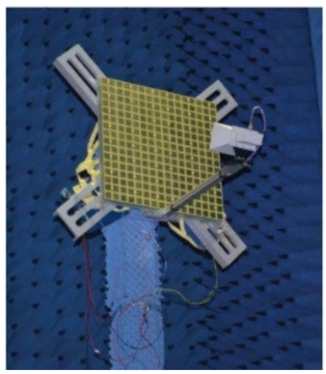

FIGURE 20. The fabricated RIS having 16 × 16.2-bit elements (images extracted from the work presented in [126]).

total of 5 PIN diodes. For four element configurations, the authors presented the phase and magnitude response of the RIS. Fig. 19(a) and Fig. 19(b) show the magnitude and phase responses of the proposed 2-bit RIS. Fig. 20 shows fabricated 16 × 16 RIS. In [127], the authors presented a mmWave PIN diode-based RIS. Fig. 21 shows the unit cell configurations of the proposed RIS. The authors rigorously studied the PIN-based metasurface and obtained a wide bandwidth around the 28 GHz frequency band. Then the authors fabricated the unit cell and verified its characteristics. Lastly, the authors fabricated 10 cm × 10 cm whole RIS and verified its performance. A rectangular WR-34 waveguide was used to measure the S-parameters of the proposed unit cell.

In [128], the authors proposed a PIN diode-based RIS working at 5.8 GHz. Computer vision was utilized to aid the RIS-based beam tracking. A camera was used to get visual information about the surrounding environment of the RIS and the information captured by the camera was used to

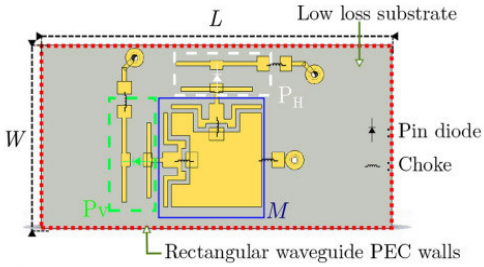

FIGURE 21. The proposed unit cell (images extracted from the work presented in [127]).

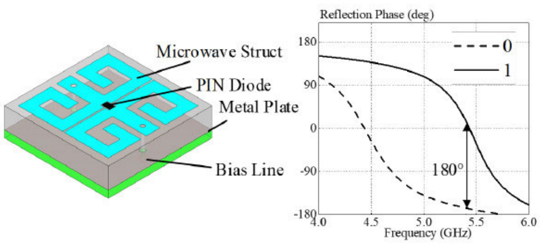

FIGURE 22. Structure diagram and modulation phase response diagram of the unit cell (images extracted from the work presented in [128]).

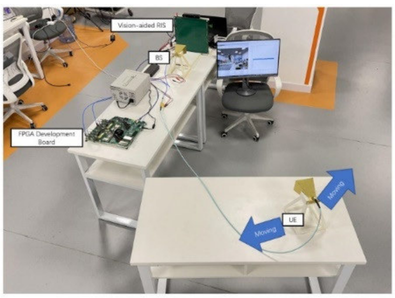

FIGURE 23. Test scenario layout (images extracted from the work presented in [128]).

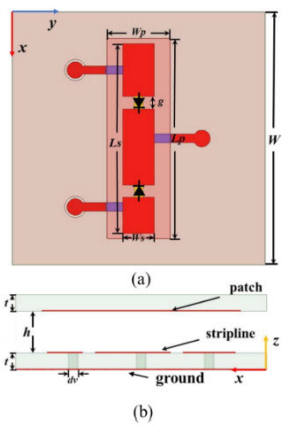

FIGURE 24. (a) Proposed top view of the 2-bit unit cell (b) side view of the unit cell (images extracted from the work presented in [129]).

reflect the beam in the desired direction. Fig. 22 shows the proposed unit cell and phase of the reflection of the proposed RIS.

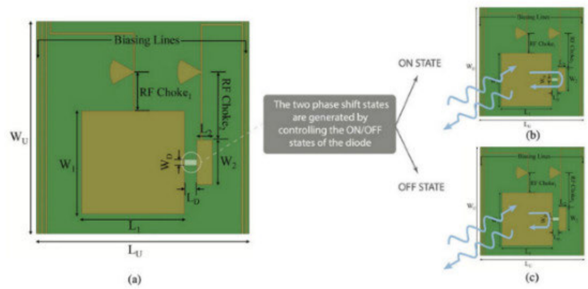

FIGURE 25. The layout of the proposed unit cell (images extracted from the work presented in [130]).

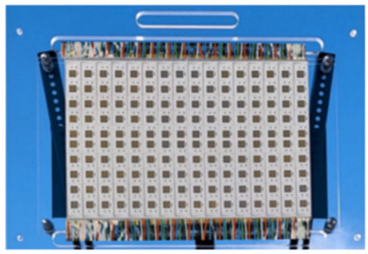

(a) RIS Front-End

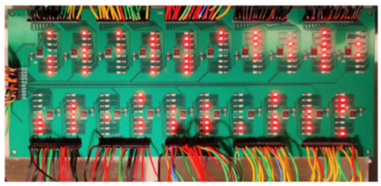

(b) RIS Back-End

FIGURE 26. (a) Top view (b) back view of the fabricated RIS (images extracted from the work presented in [130]).

A 20×20 RIS was fabricated and measured its performance using an FPGA board at 5.8 GHz to ensure a high-speed refresh of the reflection coefficient as shown in Fig. 23. Two scenarios were tested for the proposed antenna a) near field conditions where the RIS acted like a passive antenna array of the base station and b) far file conditions where the RIS assisted the exciting communication by improving the performance of the communications. Fig. 23 shows the measurement setup with the proposed RIS. A new type of 2-bit unit cell as shown in Fig. 24 was proposed in [129]. The design was very simple to realize a RIS. Another new type of RIS working at 5.8 GHz was proposed in [130]. The unit cell consists of a simple patch and a PIN diode, then a 16×10 element array was considered to get the RIS. As shown in Fig. 25, the unit cell had a 1-bit operating mechanism that had a parasite patch. Fig. 26(a) and Fig. 26(b) show the fabricated top view and bottom view of the 16×10 elements of the RIS. The authors numerically analyzed the performance of the unit cell. The magnitude of the reflection was small between the two states and the phase difference between the two states was 180° as shown in Fig. 27(a) and Fig. 27(b), respectively.

A 64-element, 2-bit high-accuracy RIS was proposed in [131], where each element could be controlled individually

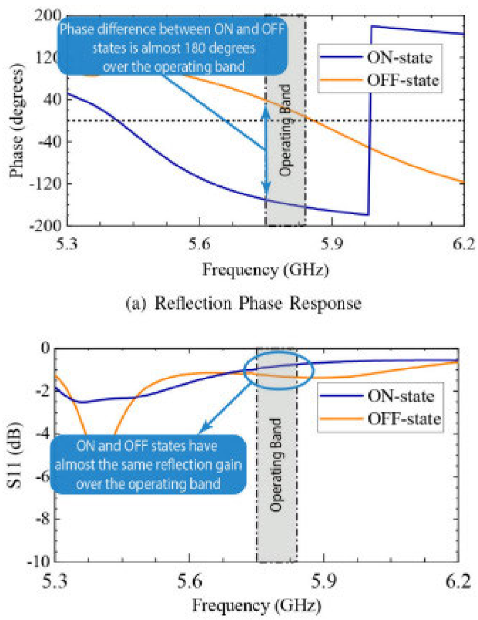

(a) Reflection Phase Response

(b) Reflection Magnitude Response

FIGURE 27. **Numerical analysis (periodic boundary conditions) of the unit cell response under boresight illumination (images extracted from the work presented in [130]).**

by using FPGA. Fig. 28 shows the measurement setup of the proposed RIS. Each unit cell had two PIN diodes and each PIN diode could be controlled by an FPGA. The proposed RIS could be deflected up to 30°.

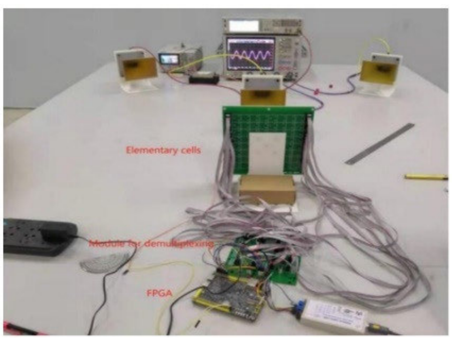

FIGURE 28. **Fabricated RIS (images extracted from the work presented in [131]).**

In [132], a 1-bit RIS was proposed to aid wireless communications to overcome path loss and shadowing. The fabricated RIS prototype is shown in Fig. 29 while Fig. 30 shows the layout of the prototype. Compress sensing-based adaptive beamforming was used. By using the proposed RIS, bit error rate (BER), and signal-to-noise ratio (SNR), were found to improve significantly.

The authors numerically analyzed the performance of the unit cell. In [133], the authors proposed an improved path-loss model suitable for RIS-aided wireless communications. The authors also fabricated RIS and the RIS consisted of 576-unit

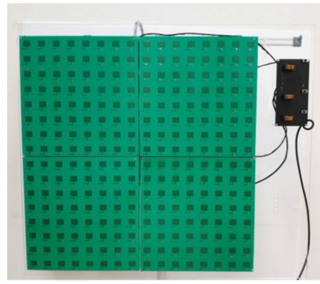

FIGURE 29. **RIS testbed (images extracted from the work presented in [132]).**

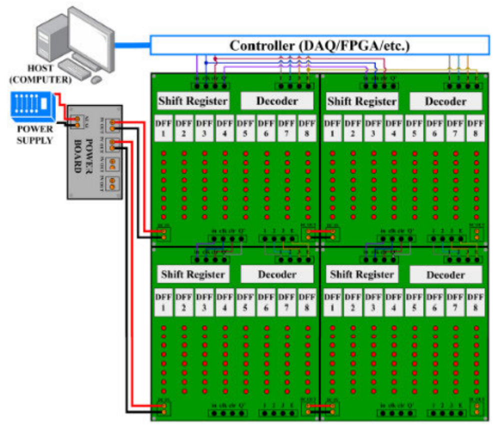

FIGURE 30. **RIS layout (images extracted from the work presented in [132]).**

cells operating at 29 GHz. Each unit cell had two PIN diodes as shown in Fig. 31. Table 4 shows the latest development of PIN diode-based RIS [126], [127], [128], [129], [130], [131], [132], [133].

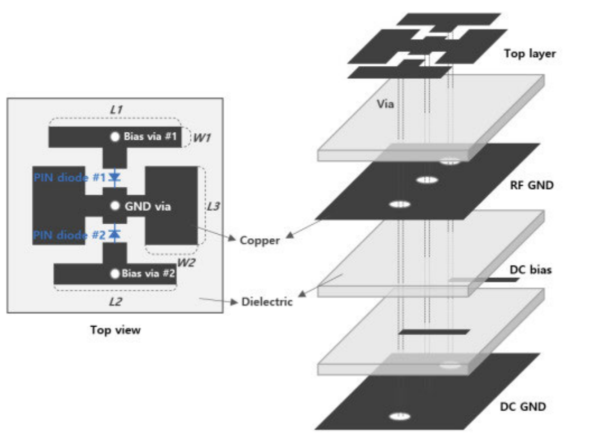

FIGURE 31. **The unit cell of the proposed RIS (images extracted from the work presented in [133]).**

D. TRANSMISSIVE RIS

Transmissive type RIS is expected to be pivotal in beyond-5G/6G communications. Reconfigurable transmitarrays are

TABLE 4. Comparison of PIN -diode-based RIS.

Ref	Unit cell type	Control mechanism	Freq.	Remarks
126	Patch	PIN diode	2.3GHz 28.5 GHz	2-bit configuration
127	Patch	PIN diode	28.5 GHz	Fabricated 10 cm ×10 cm prototype
128	Joined E-type structure	PIN diode	5.4 GHz	Computer vision was used
129	2-bit	Two PIN diodes	4.8-5.5 GHz	Only simulation results
130	Patch with parasitic patch	PIN diode	5.8 GHz	160 elements RIS
131	2-bit	PIN diode	-	High accuracy
132	Patch	PIN diode	5.8 GHz	16×16 array was used with compress sensing
133	Cross-dipole-shaped	PIN diode	29 GHz	24×24 elements RIS

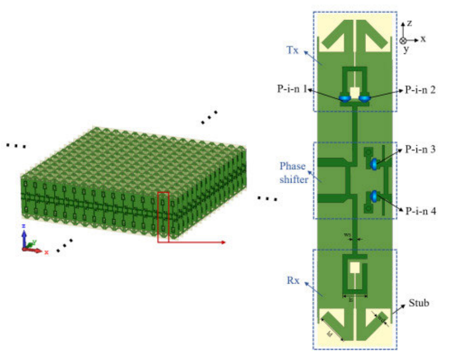

FIGURE 32. Proposed 2.5-D structure of the transmissive RIS for mmWave communications (images extracted from the work presented in [134]).

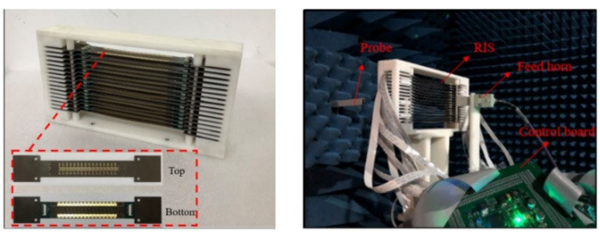

(a) (b)

FIGURE 33. Photography of (a) the fabricated transmissive RIS prototype, (b) the measurement setup in the microwave anechoic chamber.2.5-D structure of the transmissive RIS for mmWave communications (images extracted from the work presented in [134]).

the same as transmissive type RIS. For the reconfigurable transmitarray, the feeding antenna (horn or microstrip antenna array) is generally placed very close to the transmitarray.

However, it is expected that transmissive type RIS will have a feeding antenna very close as well as very large distance from the RIS. In [134], a transmissive type RIS for 6G communications was proposed. The proposed structure used a 1-bit reversible dipole and quadrature hybrid coupler-based digital phase shifter. The proposed design had 2-bit phase modulation capabilities. At 27 GHz, a maximum gain of 22 dBi was observed while the antenna was fed with a horn antenna. Fig. 32 shows the proposed unit cell of the transmissive type RIS. A prototype with 16×16 elements was fabricated and measured as shown in Fig. 33(a) and 33(b), respectively. The E-plane and H-plane radiation patterns of the proposed mmWave RIS working at 27 GHz are shown in Fig. 34. The proposed transmissive type RIS was able to scan the incoming beam in a wide range.

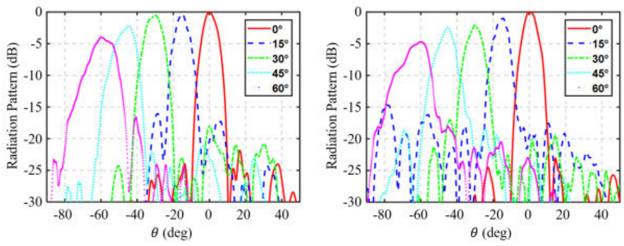

(a) (b)

FIGURE 34. Measured radiation patterns of scanned beams at 27.0 GHz in (a) E-plane, (b) H-plane (images extracted from the work presented in [134]).

E. RECONFIGURABLE INTELLIGENT SURFACE-BASED WIRELESS POWER TRANSFER

A new type of self-powered RIS was proposed in [135]. Fig. 35 shows the proposed self-powered RIS. The authors named such surface "I-Surface". The proposed surface can reconfigure the propagation environment and transfer power wirelessly to nearby devices.

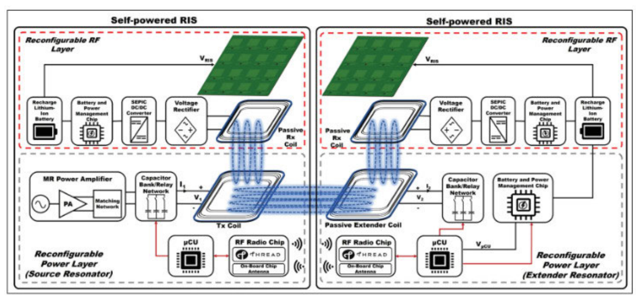

FIGURE 35. Component block diagram for self-powered RIS with reconfigurable RF and power layers (images extracted from the work presented in [135]).

RIS will be very useful to design wireless power transfer. In [136], the authors reviewed the foundations of wireless power transfer and discussed wireless power transfer in the context of RIS. In [137], the authors proposed three multi-focus techniques namely pattern addition, random unit cell interleaving, and RIS tile division for wireless power transfer using RIS.

F. 3D GRAPHENE META-ATOMS BASED RECONFIGURABLE INTELLIGENT SURFACE

A new type of 3D graphene meta-atom-based RIS was proposed in [138]. The 3D structure gave an extra degree of freedom which could improve the RIS significantly compared to its 2D counterpart. It could give extra functionalities. This new type of proposed 3D RIS will be a very promising area of research. Fig. 36 shows the proposed 3D RIS configurations. The radiation properties of the RIS could be configured by changing the state of the graphene (ON/OFF). Table 5 shows the features of transmissive type RIS, self-powered RIS, and meta-atom-based RIS [134], [135], [136], [137], [138].

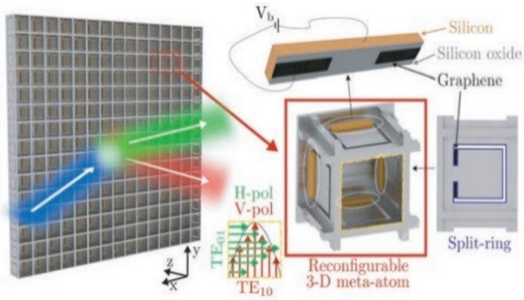

FIGURE 36. Proposed 3D IRS (images extracted from the work presented in [138]).

TABLE 5. Transmissive, self-powered, meta-atoms-based RIS.

Ref	Unit cell type	Control mechanism	Freq.	Remarks
134	Transmissive unit cell	PIN diode	27 GHz	16×16 elements RIS
135	Patch	-	5G frequency band	I-Surface was proposed
136	Rectangular patch antenna array	-	920 MHZ, 2.4 GHz, 5.8 GHz	Given an idea about modern wireless power transfer
137	1-bit unit cell	-	5.8 GHz	Use multi-focus techniques phenomena
138	3D metaatom based on graphene	On/off condition of graphene	28 GHz	3D RIS was proposed

G. 2.75-BIT, 3-BIT CODING, MULTI-BIT RECONFIGURABLE INTELLIGENT SURFACES

In [139], the authors proposed a new type of 2.75-bit RIS working at the 5G-mid-band and there was a total of 8 discrete states of the proposed design. The proposed design had 3 PIN diodes with enhanced phase resolution and a minimum number of active components. Fig. 37 (a), Fig. 37 (b) Fig. 37 (c), and Fig. 37(d) show the above view, middle layer view, cut view, and equivalent DC circuit of the proposed unit cell, respectively. To maximize the phase state separation,

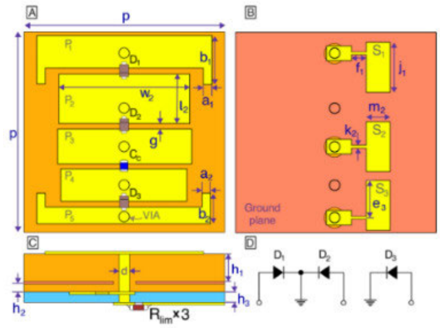

FIGURE 37. (a) Above view, (b) middle layer view (c) cut view (d) equivalent DC circuit (images extracted from the work presented in [139]).

a particle swarm optimization algorithm was employed. In [140], the authors proposed a new kind of 3-bit digital coding-based RIS. The fabricated prototype is shown in Fig. 38. The proposed structure had metal patches and varactor diodes to control the phase and amplitude of the reflected waves.

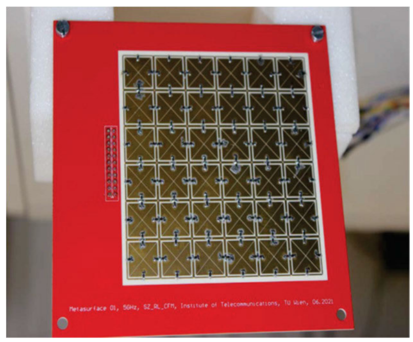

FIGURE 38. Proposed 6 × 6 RIS with varactor diodes (images extracted from the work presented in [140]).

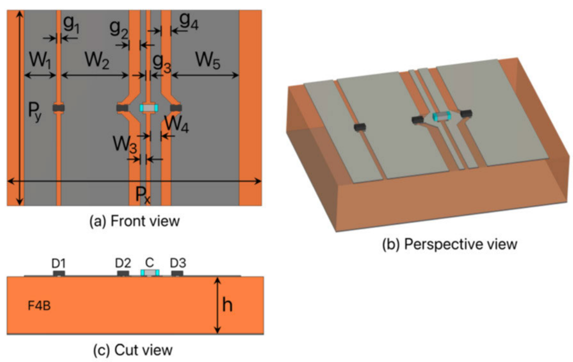

FIGURE 39. (a) Front view (b) perspective view and (c) cut view of the proposed unit cell (images extracted from the work presented in [141]).

A multi-bit PIN diode-based RIS capable of beam steering at the sub-6 GHz was proposed in [141]. An indoor field trial was carried out for different scenarios. Fig. 39(a) Fig. 39(b) and Fig. 39(c) show the front view, perspective view, and cut view of the proposed unit cell, respectively.

The authors fabricated the proposed RIS as shown in Fig. 40. Table 6 compares 2.75-bit, 3-bit, and multi-bit RISs [139], [140], [141].

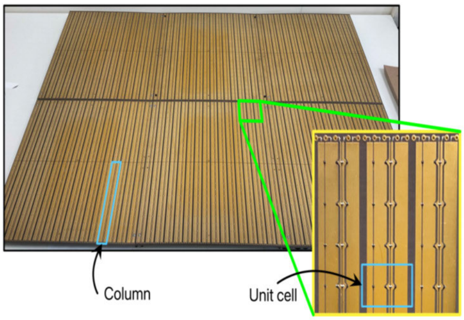

FIGURE 40. Fabricated RIS (images extracted from the work presented in [141]).

TABLE 6. 2.75 bit, 3 bit and multi-bit RIS.

Ref	Unit cell type	Control mechanism	Freq.	Remarks
139	Copper patch	PIN diode	3.75 GHz	2.75 bit
140	3-bit unit cell	Varactor diode	5 GHz	6×6 array was introduced
141	5 patches	PIN diode	3-4.5 GHz	Multi-bit operation

H. MULTI-FUNCTIONAL RECONFIGURABLE INTELLIGENT SURFACE

In the literature, there is a very limited number of hardware of multi-functional RIS available. A new type of RIS with sensing capabilities was proposed in [142]. Fig. 41 shows the proposed RIS hardware. A small portion of the impinging signal was allowed to pass through the waveguide and the collected signal was sampled by receiving circuitry. The authors were able to estimate the direction of arrival of the incoming signal in addition to the normal functions of the RIS. The proposed design is a promising design in the area of RIS. In [143] the authors proposed a sensor-integrated RIS unit cell working at the mm-Wave frequency band as shown in Fig. 42. The proposed concept is promising for the indoor environment's blind spot. A multi-functional reflective surface was proposed which can reflect the incoming signal as well as sense the surrounding environment [144]. Fig. 43 shows the proposed RIS configuration. Table 7 compares different types of multi-functional RIS [142], [143], [144].

I. RF SWITCHED-BASED RECONFIGURABLE INTELLIGENT SURFACE

In [145], the authors proposed an RF-switched-based RIS. The proposed design was based on a microstrip patch antenna, delay line, and programmable radio frequency switches without any active components. The RIS was fabricated with printed circuit board technology and low-cost components. The fabricated prototype of the proposed RIS is shown in Fig. 44.

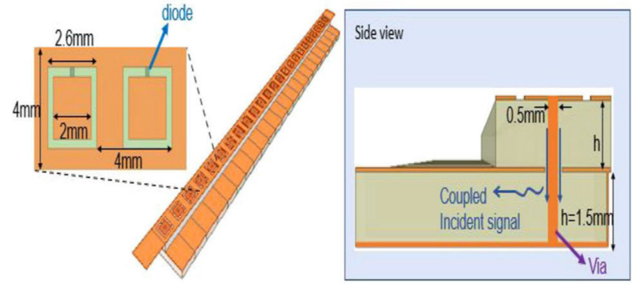

FIGURE 41. Proposed RIS with sensing capabilities (images extracted from the work presented in [142]).

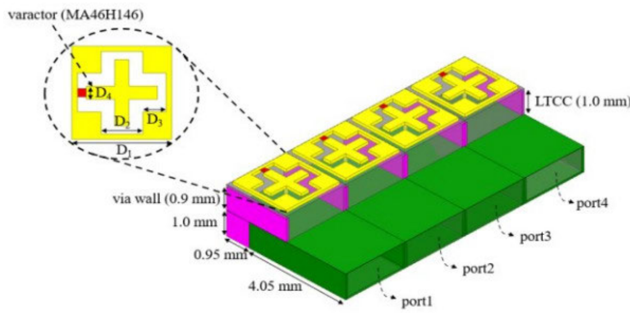

FIGURE 42. Proposed RIS with sensing capabilities (images extracted from the work presented in [143]).

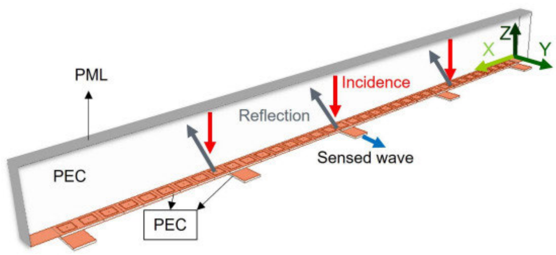

FIGURE 43. Proposed RIS with sensing capabilities (images extracted from the work presented in [144]).

TABLE 7. Multi-functional reconfigurable intelligent surface.

Ref	Unit cell type	Control mechani sm	Freq.	Remarks
142	Patch	Varactor diode	18.6-19.2 GHz	Extra sensing capabilities
143	Patch with SIW	Varactor diode	28 GHz	Sensing and beamforming capabilities
144	Mushroom structures	Varactor diode	5.8 GHz	Sensing and reconfigurable reflections

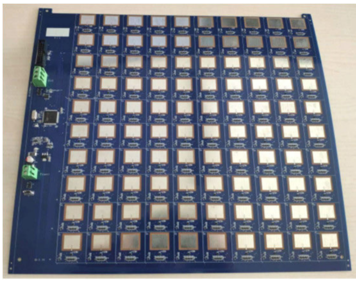

FIGURE 44. Fabricated RIS (images extracted from the work presented in [145]).

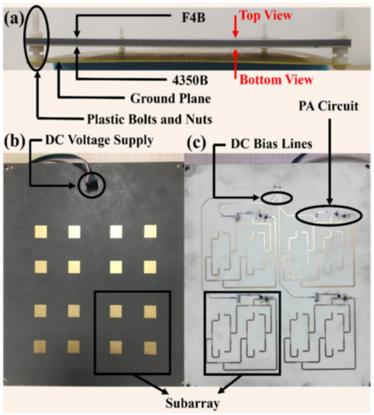

FIGURE 45. (a) Side view (b) top view (c) bottom view of the fabricated amplifying RIS (images extracted from the work presented in [146]).

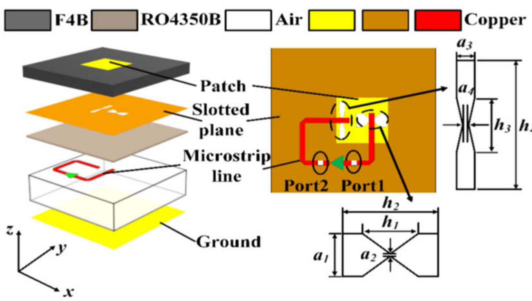

FIGURE 46. 3D view of the proposed unit cell (images extracted from the work presented in [146]).

J. AMPLIFYINGING RECONFIGURABLE INTELLIGENT SURFACE

In [146], a new type of amplifying-based RIS at the C-band was proposed, which could amplify the reflected signal by using a power amplifier. To enhance the bandwidth of the proposed structure, two orthogonal hourglass-shaped slots were conceived. Fig. 45(a), Fig. 45(b), and Fig. 45(c) show the side view, top view, and bottom view of the proposed RIS, respectively. The 3D view of the proposed unit cells is shown in Fig. 46. The unit cell had four parts (a) an upper patch layer (b) a slot plane layer (c) a microstrip line with a power amplifier (d) a ground plane.

K. VO_2-BASED RECONFIGURABLE INTELLIGENT SURFACE

There are different types of the tunning mechanism of the RIS like PIN diode, varactor diode, liquid crystal, graphene, etc. However, the authors used the metal-to-insulator property of the VO_2 to tune the RIS [147]. Fig. 47(a) and Fig. 47(b) show the diagram of differential spatial phase delay and the exploded view of the proposed unit cell, respectively. Table 8 shows features of RIS with extra sensing capabilities, RF-switch-based RIS, amplifying RIS, and VO_2 based-RIS [145], [146], [147].

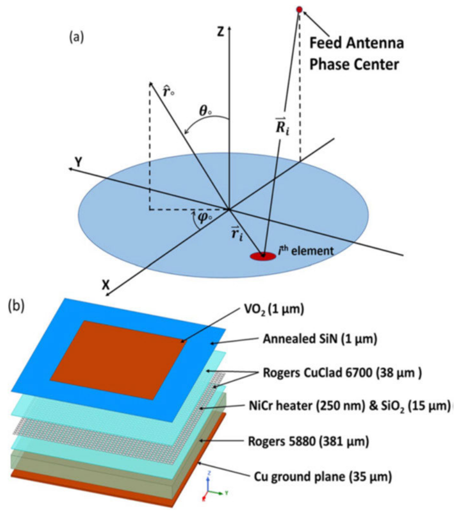

FIGURE 47. (a) Diagram of differential spatial phase delay (b) Unit cell of the RIS (images extracted from the work presented in [147]).

TABLE 8. RF switch, amplifying, and VO_2-based RIS.

Ref	Unit cell type	Control mechanism	Freq.	Remarks
145	Patch antenna	RF-switch	5.3 GHz	3D beamforming without any active component
146	Aperture coupled patch	-	5-6 GHz	Power amplifiers were used to enhance the signal strength
147	VO_2-based unit cell	VO_2	5 GHz, 32 GHz	Phase control curve covering ~ 300° and reflection loss no greater than −2 dB

L. RECONFIGURABLE INTELLIGENT SURFACE WITH RICH SCATTERING CAPABILITIES

Scattering using RIS is very important for future wideband indoor environment communications. In [79], the authors demonstrate the physical shaping of the propagation medium to get optimal channel diversity. The authors tuned the disorder and perfect orthogonality of the wireless channel was achieved using a reconfigurable metasurface placed inside a random environment. Fig. 48 shows the experimental setup for perfect channel orthogonality where a phase-binary metasurface reflect array partially covers the cavity wall.

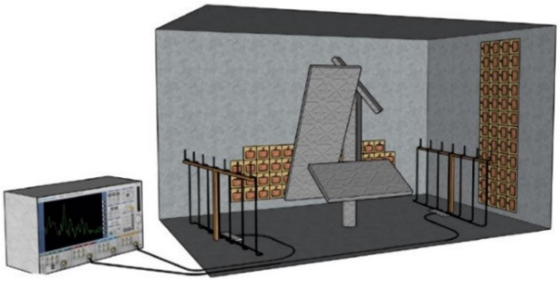

FIGURE 48. Experimental setup for perfect channel orthogonality (images extracted from the work presented in [79]).

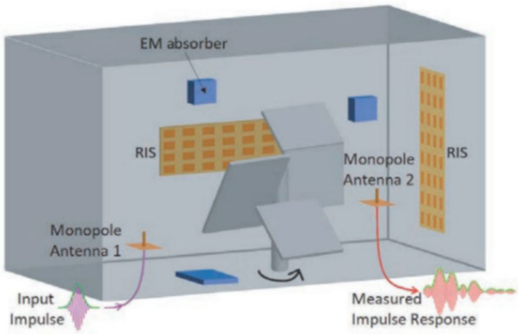

FIGURE 49. Experimental setup for one case study (images extracted from the work presented in [80]).

In [80], the authors shaped multipath channel impulse response using RIS to enable higher achievable communications rates. Also, it uses to localize non-cooperative objects using wave fingerprints. Fig. 49 shows an experimental setup that consists of an irregular metallic enclosure. The environment was very reverberant at 2.5 GHz upon excitation with a 66 MHz pulse. In [81], the authors illustrate the requirement for self-adaptive RIS under rich scattering. The authors proved that self-adaptive RISs outperform context-ignorant RISs only below particular noise levels.

M. RECONFIGURABLE INTELLIGENT SURFACE FOR INTEGRATION IN THE ON-CHIP ENVIRONMENT

In [148], initially, the authors designed and characterized a programmable metasurface for integration in the on-chip environment. Then the authors optimized the configuration to equalize selected wireless on-chip channels. Lastly, the authors noticed significantly higher modulation speeds with the shaped channel impulse response. Fig. 50 shows a metasurface programmable wireless on-chip environment.

N. PASSIVE TYPE OF RECONFIGURABLE INTELLIGENT SURFACE

In [149], the authors discussed parameters and measurement techniques for RIS. A low-cost FR4 substrate with a permittivity of 4.4 and height of 1.6 mm was taken to design the

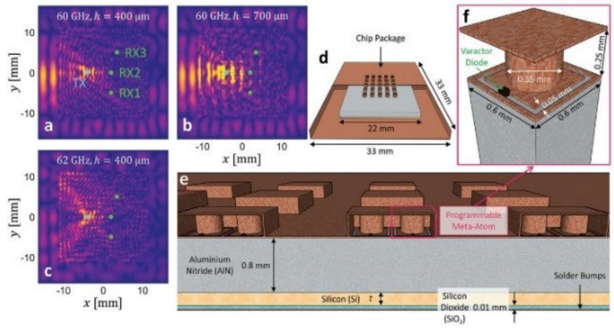

FIGURE 50. Metasurface programmable wireless on-chip environment (images extracted from the work presented in [148]).

RIS architecture. The proposed design was very simple and cost-effective. Fig. 51 shows the proposed design working at the 3.5 GHz frequency band.

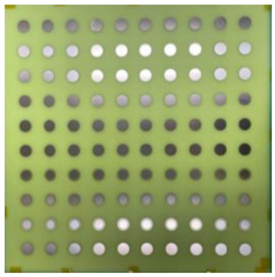

FIGURE 51. Fabricated 10 × 10 RIS (images extracted from the work presented in [149]).

O. LIQUID CRYSTAL-BASED RECONFIGURABLE INTELLIGENT SURFACE

A liquid crystal-based planar multi-resonant cell was proposed in [150]. Fig. 52 shows the reflectarray for the performance evaluations. Liquid crystal is very promising to design RIS [151], [152].

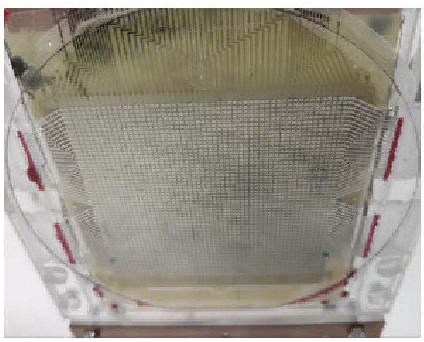

FIGURE 52. The figure of reflectarray for measurement setup (images extracted from the work presented in [150]).

It has been noticed that generally PIN didoes or varactor diodes are being used to design RIS. New types of RISs are also being considered to have sensing capabilities or new types of capabilities like the estimation of the direction of arrival of the signal.

IV. SWITCHING ELEMENTS AND MATERIALS FOR RECONFIGURABLE INTELLIGENT SURFACE

Switching of the RIS can be realized by various means like a voltage source, electric field, magnetic field, thermal variations, light, external pressure, electro-optical, etc. PIN diode and varactor diode can be tuned using an external voltage source. The RIS can have a light-sensitive material for its reconfigurability. Graphene, silicon, gallium arsenide, indium tin oxide, aluminum-doped zinc oxide, etc., are some light-sensitive materials that can be used to design RIS. Vanadium dioxide is a material that has the property of changing metal to an insulator under thermal variations. Vanadium dioxide is a very promising material to design a RIS. Transparent conducting oxides are being considered to design RIS in the near-infrared (NIR) and mid-infrared (MIR) regimes. Microfluidic can also be used as a switching element to design RIS. PIN diodes, varactor diodes, liquid crystal, MEMS switches, etc. are being considered for the potential applications of the RIS. PIN diodes and varactor diodes are inexpensive and very small in size. These can be easily integrated with the RIS surfaces. PIN and varactor diodes can work up to 30 GHz efficiently. However, at higher frequencies (above 30 GHz), PIN and varactor diodes show high insertion losses. MEMS and other mechanical-type switches are prone to failure over time due to moving parts within the switches. MEMS are expensive compared to PIN or varactor diodes. Liquid crystal is another type of potential candidate that can be used to design RIS. There may be other types of switches useful to design RIS. However, for low-cost RIS design, PIN or varactor diodes are the best to design RIS.

V. CHALLENGES AND SOLUTIONS IN HARDWARE OF RIS DESIGN

RIS is going to have a key role in beyond-5G/6G communications [153]. For such communications, the operating frequency will be not only sub-6 GHz or mmWave, but it can be THz and optical frequency band. For such deployment of RIS, the RIS should be cost-effective and simple. The cost-effective design of RIS is the fundamental challenge. It is evident from the literature reviews that nowadays maximum researchers are focusing on designing sub-6 GHz or 28 GHz frequency bands. In these frequency ranges, it is relatively easy to fabricate RIS. However, when the frequency goes beyond this, the cost to fabricate such RIS will be relatively high. Cost-effective RIS design at a higher frequency is an important issue that needs to be solved. Another important issue to design RIS is power consumption by the RIS. The RIS should consume as low as possible power for its operations. Simple configuration of the RIS is another important issue. It will be better if the reflected beam goes in the desired direction and the desired directions can vary when one user goes from one place to another place. However, it is relatively difficult to steer the beam in the desired direction when the source antenna is far from the RIS. Also, the user can come very close to RIS. So RIS should have better steering capabilities for such applications. There may be more than one user at particular locations. RIS should handle such cases. It will be better if the RIS can accept all incoming waves irrespective of their polarizations and angle of incidence. However maximum proposed RISs are not polarization-independent and those are sensitive to the angle of incidence. It is relatively difficult to design such types of RIS. These are other very important issues that need to be solved. Maintaining the perfect phase difference between the unit cells for RIS design is a very important factor. However, small manufacturing defects or other defects can change the phase difference significantly and hence the communication performance of the RIS. It is expected that RIS will have multifunctional capabilities in the future. However, the design of such multifunctional RIS is a relatively challenging task. To solve such issues, it is necessary to find new types of tuning mechanism for the unit cells which consumes less power and are cost-effective. Also, it is necessary to find new materials that can give nearly perfect reflections or nearly perfect transmission without any significant losses of power.

VI. POTENTIAL RESEARCH OR RESEARCH GAPS THAT CAN BE EXPLORED

As industry bodies are seeking cost-effective and simple RIS for the actual deployment. It is expected that different cost-effective and easy-to-fabricate RISs are going to propose in the future. Multi-functional RIS is going to play a very significant role in next-generation communications. RIS can not only reflect the beam in the desired direction but can also do other functions like sensing the incoming signal, and transmitting the signal in the desired direction, etc. Multi-functional RIS sill in the initial phase of research. Hardware for multi-functional RIS still is very limited. It is expected there will be extensive research on multi-functional RIS and different multi-functional RISs shall be proposed in near future. To improve the performance of the RIS, a new type of material needs to be proposed which can provide better tuning performance, and have a low response time, provide very low loss of the incoming signal compared to the existing materials. In [101] and [102], the authors proposed a new area of a study named ''Digital Electromagnetics'' where the electromagnetic waves were digitized for more than one function namely beam steering and polarization conversion for reconfigurable transmitarray. For that study, the feeding horn antenna was placed for a particular F/D ratio. ''Digital Electromagnetics'' is valid for both reflective types of RIS and transmissive types of RIS where the incoming waves can be digitized for more than one function such as beam steering, polarization conversion, beam shaping, etc. The advantage of this type of digitization of electromagnetic waves is that the latency for any communications can be reduced very significantly which is very important for beyond-5G/6G communications. Also, the data rate for beyond-5G/6G communications can be improved very significantly using this technique. A recent study suggests that that active types of RIS particularly sub-connected types of RIS are more useful compared to the passive types of RIS [154]. However, active-type amplifying RIS is limited in the literature. The hardware of RIS above 28 GHz is also limited. There are also some application-related areas that need to be investigated for the hardware design of the particular applications. To enhance the security of any network, RIS can enhance the secrecy rate of the wireless network. There are lots of theoretical studies in this area. However, the actual RIS design for such applications is still very limited. Wireless power transfer is going to mature in the near future. Hardware for RIS-enable wireless power transfer is still very limited. RIS-enabled wireless power transfer is expected to contribute significantly to future networks as it can wirelessly power different devices. As unmanned aerial vehicles are going to be integrated with beyond-5G/6G communications, the hardware of RIS for such applications needs to be investigated for enabling such applications. Various applications like mm-Wave communications and mobile edge computing shall also include RIS for its performance enhancement. The researchers and engineers need to design the hardware of the RIS for such applications. A new kind of RIS that can have both reflection and transmission capabilities in the desired directions is very promising. There are some theoretical works on this aspect. However, the hardware of this type of RIS still very limited.

VII. CONCLUSION

In this paper, we have reviewed extensively different types of RIS. It is evident from the current state of the art of the RIS that RIS will have a profound effect on beyond-5G/6G communications. A low-cost, self-powered RIS with multi-functional capabilities (like reflecting the beam in the desired direction, finding the direction of the arrival of the incoming signal, etc.) will be needed for future communications. RIS will be very much useful for higher frequencies communications like THz communications where it is essential to have a line of sight between transmitter and receiver. It is evident from the current state of the art of RIS, PIN diodes, and varactor diodes are being mainly used to design the RIS. However different techniques like graphene, VO_2, and liquid crystal are also very promising in designing the RIS. 1-bit RIS is being developed using PIN didoes. However, 2-bit or multi-bit RISs are also being investigated to enhance the resolution of the reflected scan beam. Nowadays maximum authors are focusing on the sub-6 GHz frequency range to design the RIS. However higher frequency ranges like 27-29 GHz range and higher are also expected to be considered for future designs. In this paper, initially, the working principles of RIS were discussed. Different type of RIS and their performance were presented. Different tables have been presented to compare the various types of RIS published in the literature. The incoming signal can be reflected by the RIS intelligently. Hence it can improve the channel capacity and increase the data rate significantly. The RIS is a promising area of research for beyond-5G/6G applications. The review paper demonstrates that instead of using a conventional massive MIMO antenna, the use of RIS is very promising for base stations. The RIS can not only be placed between the transmitter and receiver to improve the signal strength but also the RIS can be used as a transmitter or receiver itself for beyond-5G/6G applications. ‘‘Digital Electromagnetics’’ is a new area of study that needs to be considered while designing the RIS for beyond-5G/6G communications. The present authors also envision that cost-effective hardware with stable phase tuning techniques is useful for RIS design. Different types of digitally space-time coding-based metamaterial RIS are also expected to be proposed for beyond-5G/6G communications.

REFERENCES

[1] L. Subrt and P. Pechac, ‘‘Intelligent walls as autonomous parts of smart indoor environments,’’ *IET Commun.*, vol. 6, no. 8, pp. 1004–1010, May 2012.
[2] M. Giordani, M. Polese, M. Mezzavilla, S. Rangan, and M. Zorzi, ‘‘Toward 6G networks: Use cases and technologies,’’ *IEEE Commun. Mag.*, vol. 58, no. 3, pp. 55–61, Mar. 2020.
[3] K. David and H. Berndt, ‘‘6G vision and requirements: Is there any need for beyond 5G?’’ *IEEE Veh. Technol. Mag.*, vol. 13, no. 3, pp. 72–80, Sep. 2018.
[4] I. F. Akyildiz, A. Kak, and S. Nie, ‘‘6G and beyond: The future of wireless communications systems,’’ *IEEE Access*, vol. 8, pp. 133995–134030, 2020.
[5] C. Pan, H. Ren, K. Wang, J. F. Kolb, M. Elkashlan, M. Chen, M. Di Renzo, Y. Hao, J. Wang, A. L. Swindlehurst, and X. You, ‘‘Reconfigurable intelligent surfaces for 6G systems: Principles, applications, and research directions,’’ *IEEE Commun. Mag.*, vol. 59, no. 6, pp. 14–20, Jun. 2021.
[6] S. Dang, O. Amin, B. Shihada, and M.-S. Alouini, ‘‘What should 6G be?’’ *Nature Electron.*, vol. 3, no. 1, pp. 20–29, Jan. 2020.
[7] H. Viswanathan and P. E. Mogensen, ‘‘Communications in the 6G era,’’ *IEEE Access*, vol. 8, pp. 57063–57074, 2020.
[8] S. Zhang, C. Xiang, and S. Xu, ‘‘6G: Connecting everything by 1000 times price reduction,’’ *IEEE Open J. Veh. Technol.*, vol. 1, pp. 107–115, 2020.
[9] S. Chen, Y.-C. Liang, S. Sun, S. Kang, W. Cheng, and M. Peng, ‘‘Vision, requirements, and technology trend of 6G: How to tackle the challenges of system coverage, capacity, user data-rate and movement speed,’’ *IEEE Wireless Commun.*, vol. 27, no. 2, pp. 218–228, Apr. 2020.
[10] W. Jiang, B. Han, M. A. Habibi, and H. D. Schotten, ‘‘The road towards 6G: A comprehensive survey,’’ *IEEE Open J. Commun. Soc.*, vol. 2, pp. 334–366, 2021.
[11] A. Gupta and R. K. Jha, ‘‘A survey of 5G network: Architecture and emerging technologies,’’ *IEEE Access*, vol. 3, pp. 1206–1232, 2015.
[12] S. O. Oladejo and O. E. Falowo, ‘‘Latency-aware dynamic resource allocation scheme for 5G heterogeneous network: A network slicing-multitenancy scenario,’’ in *Proc. Int. Conf. Wireless Mobile Comput., Netw. Commun. (WiMob)*, Oct. 2019, pp. 1–7.
[13] M. Shafi, A. F. Molisch, P. J. Smith, T. Haustein, P. Zhu, P. De Silva, F. Tufvesson, A. Benjebbour, and G. Wunder, ‘‘5G: A tutorial overview of standards, trials, challenges, deployment, and practice,’’ *IEEE J. Sel. Areas Commun.*, vol. 35, no. 6, pp. 1201–1221, Jun. 2017.
[14] B. Rana, J.-Y. Shim, and J.-Y. Chung, ‘‘An implantable antenna with broadside radiation for a brain–machine interface,’’ *IEEE Sensors J.*, vol. 19, no. 20, pp. 9200–9205, Oct. 2019.
[15] L. Song and Y. Rahmat-Samii, ‘‘An end-to-end implanted brain–machine interface antenna system performance characterizations and development,’’ *IEEE Trans. Antennas Propag.*, vol. 65, no. 7, pp. 3399–3408, Jul. 2017.
[16] P. Bhattacharya, D. Saraswat, A. Dave, M. Acharya, S. Tanwar, G. Sharma, and I. E. Davidson, ‘‘Coalition of 6G and blockchain in AR/VR space: Challenges and future directions,’’ *IEEE Access*, vol. 9, pp. 168455–168484, 2021.
[17] S. Liao, J. Wu, J. Li, and K. Konstantin, ‘‘Information-centric massive IoT-based ubiquitous connected VR/AR in 6G: A proposed caching consensus approach,’’ *IEEE Internet Things J.*, vol. 8, no. 7, pp. 5172–5184, Apr. 2021.

[18] R. Fantacci and B. Picano, ''Edge-based virtual reality over 6G terahertz channels,'' *IEEE Netw.*, vol. 35, no. 5, pp. 28–33, Sep. 2021.

[19] X. Liu, Y. Deng, C. Han, and M. D. Renzo, ''Learning-based prediction, rendering and transmission for interactive virtual reality in RIS-assisted terahertz networks,'' *IEEE J. Sel. Areas Commun.*, vol. 40, no. 2, pp. 710–724, Feb. 2022.

[20] X. Chen, S. Leng, J. He, and L. Zhou, ''Deep-learning-based intelligent intervehicle distance control for 6G-enabled cooperative autonomous driving,'' *IEEE Internet Things J.*, vol. 8, no. 20, pp. 15180–15190, Oct. 2021.

[21] J. Zhou, D. Tian, Y. Wang, Z. Sheng, X. Duan, and V. C. M. Leung, ''Reliability-optimal cooperative communication and computing in connected vehicle systems,'' *IEEE Trans. Mobile Comput.*, vol. 19, no. 5, pp. 1216–1232, May 2020.

[22] K. Xiong, S. Leng, X. Chen, C. Huang, C. Yuen, and Y. L. Guan, ''Communication and computing resource optimization for connected autonomous driving,'' *IEEE Trans. Veh. Technol.*, vol. 69, no. 11, pp. 12652–12663, Nov. 2020.

[23] R. Shrestha, R. Bajracharya, and S. Kim, ''6G enabled unmanned aerial vehicle traffic management: A perspective,'' *IEEE Access*, vol. 9, pp. 91119–91136, 2021.

[24] R. Bajracharya, R. Shrestha, S. Kim, and H. Jung, ''6G NR-U based wireless infrastructure UAV: Standardization, opportunities, challenges and future scopes,'' *IEEE Access*, vol. 10, pp. 30536–30555, 2022.

[25] B. Shang, R. Shafin, and L. Liu, ''UAV swarm-enabled aerial reconfigurable intelligent surface (SARIS),'' *IEEE Wireless Commun.*, vol. 28, no. 5, pp. 156–163, Oct. 2021.

[26] M. Mozaffari, X. Lin, and S. Hayes, ''Toward 6G with connected sky: UAVs and beyond,'' *IEEE Commun. Mag.*, vol. 59, no. 12, pp. 74–80, Dec. 2021.

[27] S. M. R. Islam, D. Kwak, M. H. Kabir, M. Hossain, and K.-S. Kwak, ''The Internet of Things for health care: a comprehensive survey,'' *IEEE Access*, vol. 3, pp. 678–708, 2015.

[28] B. Alamri, K. Crowley, and I. Richardson, ''Blockchain-based identity management systems in health IoT: A systematic review,'' *IEEE Access*, vol. 10, pp. 59612–59629, 2022.

[29] T. Singh, A. Solanki, S. K. Sharma, A. Nayyar, and A. Paul, ''A decade review on smart cities: Paradigms, challenges and opportunities,'' *IEEE Access*, vol. 10, pp. 68319–68364, 2022.

[30] J. Yang, Y. Kwon, and D. Kim, ''Regional smart city development focus: the South Korean national strategic smart city program,'' *IEEE Access*, vol. 9, pp. 7193–7210, 2021.

[31] E. Sippel, J. Geiss, S. Bruckner, P. Groschel, M. Hehn, and M. Vossiek, ''Exchanging bandwidth with aperture size in wireless indoor localization—Or why 5G/6G systems with antenna arrays can outperform UWB solutions,'' *IEEE Open J. Veh. Technol.*, vol. 2, pp. 207–217, 2021.

[32] S. Fan, Y. Wu, C. Han, and X. Wang, ''SIABR: A structured intra-attention bidirectional recurrent deep learning method for ultra-accurate terahertz indoor localization,'' *IEEE J. Sel. Areas Commun.*, vol. 39, no. 7, pp. 2226–2240, Jul. 2021.

[33] Z. Zhang, Y. Xiao, Z. Ma, M. Xiao, Z. Ding, X. Lei, G. K. Karagiannidis, and P. Fan, ''6G wireless networks: Vision, requirements, architecture, and key technologies,'' *IEEE Veh. Technol. Mag.*, vol. 14, no. 3, pp. 28–41, Sep. 2019.

[34] W. Saad, M. Bennis, and M. Chen, ''A vision of 6G wireless systems: Applications, trends, technologies, and open research problems,'' *IEEE Netw.*, vol. 34, no. 3, pp. 134–142, May 2020.

[35] K. B. Letaief, W. Chen, Y. Shi, J. Zhang, and Y. A. Zhang, ''The roadmap to 6G: AI empowered wireless networks,'' *IEEE Commun. Mag.*, vol. 57, no. 8, pp. 84–90, Aug. 2019.

[36] W. Tang, M. Z. Chen, J. Y. Dai, Y. Zeng, X. Zhao, S. Jin, Q. Cheng, and T. J. Cui, ''Wireless communications with programmable metasurface: New paradigms, opportunities, and challenges on transceiver design,'' *IEEE Wireless Commun.*, vol. 27, pp. 180–187, 2020.

[37] S. Gong, X. Lu, D. T. Hoang, D. Niyato, L. Shu, D. I. Kim, and Y. C. Liang, ''Toward smart wireless communications via intelligent reflecting surfaces: A contemporary survey,'' *IEEE Commun. Surveys Tuts.*, vol. 22, no. 4, pp. 2283–2314, 4th Quart., 2020.

[38] F. C. Okogbaa, Q. Z. Ahmed, F. A. Khan, W. B. Abbas, F. Che, S. A. R. Zaidi, and T. Alade, ''Design and application of intelligent reflecting surface (IRS) for beyond 5G wireless networks: A review,'' *Sensors*, vol. 22, no. 7, p. 2436, 2022.

[39] Y. Liu, X. Liu, X. Mu, T. Hou, J. Xu, M. Di Renzo, and N. Al-Dhahir, ''Reconfigurable intelligent surfaces: Principles and opportunities,'' *IEEE Commun. Surveys Tuts.*, vol. 23, no. 3, pp. 1546–1577, 3rd Quart., 2021.

[40] M. Di Renzo, A. Zappone, M. Debbah, M. S. Alouini, C. Yuen, J. De Rosny, and S. Tretyakov, ''Smart radio environments empowered by reconfigurable intelligent surfaces: How it works, state of research, and the road ahead,'' *IEEE J. Sel. Areas Commun.*, vol. 38, no. 11, pp. 2450–2525, Jul. 2020.

[41] B. Ning, Z. Chen, W. Chen, and J. Fang, ''Beamforming optimization for intelligent reflecting surface assisted MIMO: A sum-path-gain maximization approach,'' *IEEE Wireless Commun. Lett.*, vol. 9, no. 7, pp. 1105–1109, Jul. 2020.

[42] S. Sugiura, Y. Kawai, T. Matsui, T. Lee, and H. Iizuka, ''Joint beam and polarization forming of intelligent reflecting surfaces for wireless communications,'' *IEEE Trans. Veh. Technol.*, vol. 70, no. 2, pp. 1648–1657, Feb. 2021.

[43] B. Di, H. Zhang, L. Song, Y. Li, Z. Han, and H. V. Poor, ''Hybrid beamforming for reconfigurable intelligent surface based multi-user communications: Achievable rates with limited discrete phase shifts,'' *IEEE J. Sel. Areas Commun.*, vol. 38, no. 8, pp. 1809–1822, Aug. 2020.

[44] Q. Q. Wu and R. Zhang, ''Beamforming optimization for wireless network aided by intelligent reflecting surface with discrete phase shifts,'' *IEEE Trans. Commun.*, vol. 68, no. 3, pp. 1838–1851, May 2020.

[45] Q. Wu and R. Zhang, ''Joint active and passive beamforming optimization for intelligent reflecting surface assisted SWIPT under QoS constraints,'' *IEEE J. Sel. Areas Commun.*, vol. 38, no. 8, pp. 1735–1748, Aug. 2020.

[46] C. You, B. Zheng, and R. Zhang, ''Channel estimation and passive beamforming for intelligent reflecting surface: Discrete phase shift and progressive refinement,'' *IEEE J. Sel. Areas Commun.*, vol. 38, no. 11, pp. 2604–2620, Nov. 2020.

[47] Q. Wu and R. Zhang, ''Intelligent reflecting surface enhanced wireless network via joint active and passive beamforming,'' *IEEE Trans. Wireless Commun.*, vol. 18, no. 11, pp. 5394–5409, Nov. 2019.

[48] O. Yurduseven, S. D. Assimonis, and M. Matthaiou, ''Intelligent reflecting surfaces with spatial modulation: An electromagnetic perspective,'' *IEEE Open J. Commun. Soc.*, vol. 1, pp. 1256–1266, 2020.

[49] H. Yang, Z. Xiong, J. Zhao, D. Niyato, L. Xiao, and Q. Wu, ''Deep reinforcement learning-based intelligent reflecting surface for secure wireless communications,'' *IEEE Trans. Wireless Commun.*, vol. 20, no. 1, pp. 375–388, Jan. 2021.

[50] B. Sheen, J. Yang, X. Feng, and M. M. U. Chowdhury, ''A deep learning based modeling of reconfigurable intelligent surface assisted wireless communications for phase shift configuration,'' *IEEE Open J. Commun. Soc.*, vol. 2, pp. 262–272, 2021.

[51] V. P. Tuan and I. P. Hong, ''Secrecy performance analysis and optimization of intelligent reflecting surface-aided indoor wireless communications,'' *IEEE Access*, vol. 8, pp. 109440–109452, 2020.

[52] C. Huang, A. Zappone, G. C. Alexandropoulos, M. Debbah, and C. Yuen, ''Reconfigurable intelligent surfaces for energy efficiency in wireless communication,'' *IEEE Trans. Wireless Commun.*, vol. 18, no. 8, pp. 4157–4170, Aug. 2019.

[53] C. You, B. Zheng, and R. Zhang, ''Wireless communication via double IRS: Channel estimation and passive beamforming designs,'' *IEEE Wireless Commun. Lett.*, vol. 10, no. 2, pp. 431–435, Feb. 2021.

[54] E. Bjornson, O. Ozdogan, and E. G. Larsson, ''Reconfigurable intelligent surfaces: Three myths and two critical questions,'' *IEEE Commun. Mag.*, vol. 58, no. 12, pp. 90–96, Jan. 2021.

[55] W. Tang, M. Z. Chen, X. Chen, J. Y. Dai, Y. Han, M. Di Renzo, Y. Zeng, S. Jin, Q. Cheng, and T. J. Cui, ''Wireless communications with reconfigurable intelligent surface: Path loss modeling and experimental measurement,'' *IEEE Trans. Wireless Commun.*, vol. 20, no. 1, pp. 421–439, Jan. 2021.

[56] M. A. El Mossallamy, H. Zhang, L. Song, K. G. Seddik, Z. Han, and G. Y. Li, ''Reconfigurable intelligent surfaces for wireless communications: Principles, challenges, and opportunities,'' *IEEE Trans. Cogn. Commun. Netw.*, vol. 6, no. 3, pp. 990–1002, Sep. 2020.

[57] X. Yuan, Y.-J. A. Zhang, Y. Shi, W. Yan, and H. Liu, ''Reconfigurable intelligent-surface empowered wireless communications: Challenges and opportunities,'' *IEEE Wireless Commun.*, vol. 28, no. 2, pp. 136–143, Apr. 2021.

[58] S. Li, B. Duo, M. D. Renzo, M. Tao, and X. Yuan, ''Robust secure UAV communications with the aid of reconfigurable intelligent surfaces,'' *IEEE Trans. Wireless Commun.*, vol. 20, no. 10, pp. 6402–6417, Apr. 2021.

[59] E. Basar, M. Di Renzo, J. De Rosny, M. Debbah, M.-S. Alouini, and R. Zhang, "Wireless communications through reconfigurable intelligent surfaces," *IEEE Access*, vol. 7, pp. 116753–116773, 2019.

[60] M. H. Khoshafa, T. M. N. Ngatched, M. H. Ahmed, and A. R. Ndjiongue, "Active reconfigurable intelligent surfaces-aided wireless communication system," *IEEE Commun. Lett.*, vol. 25, no. 11, pp. 3699–3703, Nov. 2021.

[61] H. Wymeersch, J. He, B. Denis, A. Clemente, and M. Juntti, "Radio localization and mapping with reconfigurable intelligent surfaces: Challenges, opportunities, and research directions," *IEEE Veh. Technol. Mag.*, vol. 15, no. 4, pp. 52–61, Dec. 2020.

[62] X. Guo, Y. Chen, and Y. Wang, "Learning-based robust and secure transmission for reconfigurable intelligent surface aided millimeter wave UAV communications," *IEEE Wireless Commun. Lett.*, vol. 10, no. 8, pp. 1795–1799, Aug. 2021.

[63] A. Papazafeiropoulos, C. Pan, A. Elbir, P. Kourtessis, S. Chatzinotas, and J. M. Senior, "Coverage probability of distributed IRS systems under spatially correlated channels," *IEEE Wireless Commun. Lett.*, vol. 10, no. 8, pp. 1722–1726, Aug. 2021.

[64] Q. Wu and R. Zhang, "Towards smart and reconfigurable environment: Intelligent reflecting surface aided wireless network," *IEEE Commun. Mag.*, vol. 58, no. 1, pp. 106–112, Jan. 2020.

[65] X. Yu, D. Xu, Y. Sun, D. W. K. Ng, and R. Schober, "Robust and secure wireless communications via intelligent reflecting surfaces," *IEEE J. Sel. Areas Commun.*, vol. 38, no. 11, pp. 2637–2652, Nov. 2020.

[66] Ö. Özdogan, E. Björnson, and E. G. Larsson, "Intelligent reflecting surfaces: Physics, propagation, and pathloss modeling," *IEEE Wireless Commun. Lett.*, vol. 9, no. 5, pp. 581–585, Dec. 2019.

[67] A. S. D. Sena, D. Carrillo, F. Fang, P. H. Nardelli, D. B. Da Costa, U. S. Dias, Z. Ding, C. B. Papadias, and W. Saad, "What role do intelligent reflecting surfaces play in multi-antenna non-orthogonal multiple access?" *IEEE Wireless Commun.*, vol. 27, no. 5, pp. 24–31, Oct. 2020.

[68] P. Wang, J. Fang, H. Duan, and H. Li, "Compressed channel estimation for intelligent reflecting surface-assisted millimeter wave systems," *IEEE Signal Process. Lett.*, vol. 27, pp. 905–909, 2020.

[69] M. Cui, G. Zhang, and R. Zhang, "Secure wireless communication via intelligent reflecting surface," *IEEE Wireless Commun. Lett.*, vol. 8, no. 5, pp. 1410–1414, Oct. 2019.

[70] C. Pan, H. Ren, K. Wang, M. Elkashlan, A. Nallanathan, J. Wang, and L. Hanzo, "Intelligent reflecting surface enhanced MIMO broadcasting for simultaneous wireless information and power transfer," *IEEE J. Sel. Areas Commun.*, vol. 38, no. 8, pp. 1719–1734, Aug. 2020.

[71] J. Yuan, Y.-C. Liang, J. Joung, G. Feng, and E. G. Larsson, "Intelligent reflecting surface-assisted cognitive radio system," *IEEE Trans. Commun.*, vol. 69, no. 1, pp. 675–687, Jan. 2021.

[72] X. Ma, Z. Chen, W. Chen, Z. Li, Y. Chi, C. Han, and S. Li, "Joint channel estimation and data rate maximization for intelligent reflecting surface assisted terahertz MIMO communication systems," *IEEE Access*, vol. 8, pp. 99565–99581, 2020.

[73] M. Jung, W. Saad, and G. Kong, "Performance analysis of active large intelligent surfaces (LISs): Uplink spectral efficiency and pilot training," *IEEE Trans. Commun.*, vol. 69, no. 5, pp. 3379–3394, May 2021.

[74] F.-L. Jin, X. Ding, Y.-F. Cheng, B.-Z. Wang, and W. Shao, "A wideband phased array with broad scanning range and wide-angle impedance matching," *IEEE Trans. Antennas Propag.*, vol. 68, no. 8, pp. 6022–6031, Aug. 2020.

[75] Y. Q. Wen, B. Z. Wang, and X. Ding, "A wide-angle scanning and low sidelobe level microstrip phased array based on genetic algorithm optimization," *IEEE Trans. Antennas Propag.*, vol. 64, no. 2, pp. 805–810, Feb. 2016.

[76] B. A. Arand, A. Bazrkar, and A. Zahedi, "Design of a phased array in triangular grid with an efficient matching network and reduced mutual coupling for wide-angle scanning," *IEEE Trans. Antennas Propag.*, vol. 65, no. 6, pp. 2983–2991, Jun. 2017.

[77] Y.-Q. Wen, S. Gao, B.-Z. Wang, and Q. Luo, "Dual-polarized and wide-angle scanning microstrip phased array," *IEEE Trans. Antennas Propag.*, vol. 66, no. 7, pp. 3775–3780, Jul. 2018.

[78] G. Yang, Q. Chen, J. Li, S. Zhou, and Z. Xing, "Improving wide-angle scanning performance of phased array antenna by dielectric sheet," *IEEE Access*, vol. 7, pp. 71897–71906, 2019.

[79] P. Del Hougne, M. Fink, and G. Lerosey, "Optimally diverse communication channels in disordered environments with tuned randomness," *Nature Electron.*, vol. 2, no. 1, pp. 36–41, 2019.

[80] G. C. Alexandropoulos, N. Shlezinger, and P. Del Hougne, "Reconfigurable intelligent surfaces for rich scattering wireless communications: Recent experiments, challenges, and opportunities," *IEEE Commun. Mag.*, vol. 59, no. 6, pp. 28–34, Jun. 2021.

[81] C. Saigre-Tardif and P. Del Hougne, "Self-adaptive RISs beyond free space: Convergence of localization, sensing and communication under rich-scattering conditions," 2022, *arXiv:2205.11186*.

[82] I. J. Nam, S. M. Lee, and D. H. Kim, "Miniaturized beam reconfigurable reflectarray antenna with wide 3-D beam coverage," *IEEE Trans. Antennas Propag.*, vol. 70, no. 4, pp. 2613–2622, Apr. 2022.

[83] B. J. Xiang, X. Dai, and K.-M. Luk, "A wideband low-cost reconfigurable reflectarray antenna with 1-bit resolution," *IEEE Trans. Antennas Propag.*, vol. 70, no. 9, pp. 7439–7447, Sep. 2022.

[84] H. Yang, F. Yang, X. Cao, S. Xu, J. Gao, X. Chen, M. Li, and T. Li, "A 1600-element dual-frequency electronically reconfigurable reflectarray at X/Ku-band," *IEEE Trans. Antennas Propag.*, vol. 65, no. 6, pp. 3024–3032, Jun. 2017.

[85] J. Han, L. Li, G. Liu, Z. Wu, and Y. Shi, "A wideband 1 bit 12 × 12 reconfigurable beam-scanning reflectarray: Design, fabrication, and measurement," *IEEE Antennas Wireless Propag. Lett.*, vol. 18, no. 6, pp. 1268–1272, Jun. 2019.

[86] H. Zhang, X. Chen, Z. Wang, Y. Ge, and J. Pu, "A 1-bit electronically reconfigurable reflectarray antenna in X band," *IEEE Access*, vol. 7, pp. 66567–66575, 2019.

[87] Z. Wang, Y. Ge, J. Pu, X. Chen, G. Li, Y. Wang, K. Liu, H. Zhang, and Z. Chen, "1 bit electronically reconfigurable folded reflectarray antenna based on p-i-n diodes for wide-angle beam-scanning applications," *IEEE Trans. Antennas Propag.*, vol. 68, no. 9, pp. 6806–6810, Sep. 2020.

[88] P. Mei, Y. Cai, K. Zhao, Z. Ying, G. F. Pedersen, X. Q. Lin, and S. Zhang, "On the study of reconfigurable intelligent surfaces in the near-field region," *IEEE Trans. Antennas Propag.*, vol. 70, no. 10, pp. 8718–8728, Oct. 2022.

[89] A. Wagle and S. Vrudhula, "Heterogeneous FPGA architecture using threshold logic gates for improved area, power, and performance," *IEEE Trans. Comput.-Aided Design Integr. Circuits Syst.*, vol. 41, no. 6, pp. 1855–1867, Jun. 2022.

[90] B. Yang, Z. Yu, J. Lan, R. Zhang, J. Zhou, and W. Hong, "Digital beamforming-based massive MIMO transceiver for 5G millimeter-wave communications," *IEEE Trans. Microw. Theory Techn.*, vol. 66, no. 7, pp. 3403–3418, Jul. 2018.

[91] L. Kuai, J. Chen, Z. H. Jiang, C. Yu, C. Guo, Y. Yu, H. X. Zhou, and W. Hong, "A N260 band 64 channel millimeter wave full-digital multi-beam array for 5G massive MIMO applications," *IEEE Access*, vol. 8, pp. 47640–47653, 2020.

[92] A. Clemente, L. Dussopt, R. Sauleau, P. Potier, and P. Pouliguen, "1-bit reconfigurable unit cell based on PIN diodes for transmit-array applications in X band," *IEEE Trans. Antennas Propag.*, vol. 60, no. 5, pp. 2260–2269, May 2012.

[93] A. Clemente, L. Dussopt, R. Sauleau, P. Potier, and P. Pouliguen, "Wideband 400-element electronically reconfigurable transmitarray in X-band," *IEEE Trans. Antennas Propag.*, vol. 61, no. 10, pp. 5017–5027, Oct. 2013.

[94] M. Wang, S. Xu, F. Yang, and M. Li, "Design and measurement of a 1-bit reconfigurable transmitarray with subwavelength H-shaped coupling slot elements," *IEEE Trans. Antennas Propag.*, vol. 67, no. 5, pp. 3500–3504, May 2019.

[95] W. Pan, C. Huang, X. Ma, B. Jiang, and X. Luo, "A dual linearly polarized transmitarray element with 1-bit phase resolution in X-band," *IEEE Antennas Wireless Propag. Lett.*, vol. 14, pp. 167–170, 2015.

[96] C. Huang, W. Pan, X. Ma, and X. Luo, "1 bit reconfigurable circularly polarized transmit-array in X-band," *IEEE Antennas Wireless Propag. Lett.*, vol. 15, pp. 448–451, 2015.

[97] P. Padilla, A. Muñoz-Acevedo, M. Sierra-Castaner, and M. Sierra-Perez, "Electronically reconfigurable transmitarray at Ku band for microwave applications," *IEEE Trans. Antennas Propag.*, vol. 58, no. 8, pp. 2571–2579, Aug. 2010.

[98] J. Y. Lau and S. V. Hum, "Analysis and characterization of a multipole reconfigurable transmitarray element," *IEEE Trans. Antennas Propag.*, vol. 59, no. 1, pp. 70–79, Jan. 2011.

[99] J. Y. Lau and S. V. Hum, "Reconfigurable transmitarray design approaches for beamforming applications," *IEEE Trans. Antennas Propag.*, vol. 60, no. 12, pp. 5679–5689, Dec. 2012.

[100] B. Rana, I.-G. Lee, and I.-P. Hong, "Experimental characterization of 2 × 2 electronically reconfigurable 1 bit unit cells for a beamforming transmitarray at X band," *J. Electromagn. Eng. Sci.*, vol. 21, no. 2, pp. 153–160, Apr. 2021.

[101] B. Rana, I.-G. Lee, and I.-P. Hong, "Digitally reconfigurable transmitarray with beam-steering and polarization switching capabilities," *IEEE Access*, vol. 9, pp. 144140–144148, 2021.

[102] B. Rana, I.-G. Lee, and I.-P. Hong, "A 4×4 digitally reconfigurable transmitarray: Measurement of radiation patterns," *IEICE Electron. Exp.*, vol. 19, no. 4, 2021, Art. no. 20210550.

[103] S. V. Hum and J. Perruisseau-Carrier, "Reconfigurable reflectarrays and array lenses for dynamic antenna beam control: A review," *IEEE Trans. Antennas Propag.*, vol. 62, no. 1, pp. 183–198, Jan. 2014.

[104] E. Carrasco, M. Barba, and J. A. Encinar, "X-band reflectarray antenna with switching-beam using PIN diodes and gathered elements," *IEEE Trans. Antennas Propag.*, vol. 60, no. 12, pp. 5700–5708, Dec. 2012.

[105] H. Yang, F. Yang, S. Xu, Y. Mao, M. Li, X. Cao, and J. Gao, "A 1-bit 10 × 10 reconfigurable reflectarray antenna: Design, optimization, and experiment," *IEEE Trans. Antennas Propag.*, vol. 64, no. 6, pp. 2246–2254, Jun. 2016.

[106] C. L. Holloway, E. F. Kuester, J. A. Gordon, J. O'Hara, J. Booth, and D. R. Smith, "An overview of the theory and applications of metasurfaces: The two-dimensional equivalents of metamaterials," *IEEE Antenn. Propag. Mag.*, vol. 54, no. 4, pp. 10–35, Jul. 2012.

[107] M. D. Renzo, M. Debbah, D.-T. Phan-Huy, A. Zappone, M.-S. Alouini, C. Yuen, V. Sciancalepore, G. C. Alexandropoulos, J. Hoydis, H. Gacanin, J. D. Rosny, A. Bounceur, G. Lerosey, and M. Fink, "Smart radio environments empowered by reconfigurable AI meta-surfaces: An idea whose time has come," *EURASIP J. Wireless Commun. Netw.*, vol. 2019, no. 1, pp. 1–20, May 2019.

[108] Q. Wu, S. Zhang, B. Zheng, C. You, and R. Zhang, "Intelligent reflecting surface-aided wireless communications: A tutorial," *IEEE Trans. Commun.*, vol. 69, no. 5, pp. 3313–3351, May 2021.

[109] Y.-C. Liang, R. Long, Q. Zhang, J. Chen, H. V. Cheng, and H. Guo, "Large intelligent surface/antennas (LISA): Making reflective radios smart," *J. Commun. Inf. Netw.*, vol. 4, no. 2, pp. 40–50, Jun. 2019.

[110] Y. Saifullah, Y. He, A. Boag, G. Yang, and F. Xu, "Recent progress in reconfigurable and intelligent metasurfaces: A comprehensive review of tuning mechanisms, hardware designs, and applications," *Adv. Sci.*, vol. 9, no. 33, Nov. 2022, Art. no. 2203747.

[111] S. R. Rengarajan and Y. Rahmat-Samii, "The field equivalence principle: Illustration of the establishment of the non-intuitive null fields," *IEEE Antennas Propag. Mag.*, vol. 42, no. 4, pp. 122–128, Aug. 2000.

[112] B. O. Zhu, K. Chen, N. Jia, L. Sun, J. Zhao, T. Jiang, and Y. Feng, "Dynamic control of electromagnetic wave propagation with the equivalent principle inspired tunable metasurface," *Sci. Rep.*, vol. 4, no. 1, pp. 1–7, 2014.

[113] R. Faqiri, C. Saigre-Tardif, G. C. Alexandropoulos, N. Shlezinger, M. F. Imani, and P. Del Hougne, "PhysFad: Physics-based end-to-end channel modeling of RIS-parametrized environments with adjustable fading," *IEEE Trans. Wireless Commun.*, vol. 22, no. 1, pp. 580–595, Jan. 2023.

[114] G. Gradoni and M. Di Renzo, "End-to-end mutual coupling aware communication model for reconfigurable intelligent surfaces: An electromagnetic-compliant approach based on mutual impedances," *IEEE Wireless Commun. Lett.*, vol. 10, no. 5, pp. 938–942, May 2021.

[115] M. D. Pozar, *Microwave Engineering*, 4th ed. Hoboken, NJ, USA: Wiley, 2012.

[116] C. L. Holloway, M. A. Mohamed, E. F. Kuester, and A. Dienstfrey, "Reflection and transmission properties of a metafilm: With an application to a controllable surface composed of resonant particles," *IEEE Trans. Antennas Propag.*, vol. 47, no. 4, pp. 853–865, Nov. 2005.

[117] H. Kamoda, T. Iwasaki, J. Tsumochi, T. Kuki, and O. Hashimoto, "60-GHz electronically reconfigurable large reflectarray using single-bit phase shifters," *IEEE Trans. Antennas Propag.*, vol. 59, no. 7, pp. 2524–2531, Jul. 2011.

[118] T. J. Cui, M. Q. Qi, X. Wan, J. Zhao, and Q. Cheng, "Coding metamaterials, digital metamaterials and programmable metamaterials," *Light, Sci. Appl.*, vol. 3, no. 10, p. 218, Oct. 2014.

[119] N. Kaina, M. Dupré, M. Fink, and G. Lerosey, "Hybridized resonances to design tunable binary phase metasurface unit cells," *Opt. Exp.*, vol. 22, no. 16, pp. 18881–18888, 2014.

[120] R. G. Meyer and M. L. Stephens, "Distortion in variable-capacitance diodes," *IEEE J. Solid-State Circuits*, vol. SSC-10, no. 1, pp. 47–54, Feb. 1975.

[121] D. F. Sievenpiper, J. H. Schaffner, H. J. Song, R. Y. Loo, and G. Tangonan, "Two-dimensional beam steering using an electrically tunable impedance surface," *IEEE Trans. Antennas Propag.*, vol. 51, no. 10, pp. 2713–2722, Oct. 2003.

[122] A. Araghi, M. Khalily, M. Safaei, A. Bagheri, V. Singh, F. Wang, and R. Tafazolli, "Reconfigurable intelligent surface (RIS) in the sub-6 GHz band: Design, implementation, and real-world demonstration," *IEEE Access*, vol. 10, pp. 2646–2655, 2022.

[123] X. Pei, H. Yin, L. Tan, L. Cao, Z. Li, K. Wang, K. Zhang, and E. Bjornson, "RIS-aided wireless communications: Prototyping, adaptive beamforming, and indoor/outdoor field trials," *IEEE Trans. Commun.*, vol. 69, no. 12, pp. 8627–8640, Dec. 2021.

[124] L. G. Da Silva and P. Xiao, "A 2-bit tunable unit cell for 6G reconfigurable intelligent surface application," in *Proc. 16th Eur. Conf. Antennas Propag. (EuCAP)*, Mar. 2022, pp. 1–5.

[125] R. Fara, P. Ratajczak, D.-T. Phan-Huy, A. Ourir, M. Di Renzo, and J. De Rosny, "A prototype of reconfigurable intelligent surface with continuous control of the reflection phase," *IEEE Wireless Commun.*, vol. 29, no. 1, pp. 70–77, Feb. 2022.

[126] L. Dai, B. Wang, M. Wang, X. Yang, J. Tan, S. Bi, S. Xu, F. Yang, Z. Chen, M. D. Renzo, C.-B. Chae, and L. Hanzo, "Reconfigurable intelligent surface-based wireless communications: Antenna design, prototyping, and experimental results," *IEEE Access*, vol. 8, pp. 45913–45923, 2020.

[127] J.-B. Gros, V. Popov, M. A. Odit, V. Lenets, and G. Lerosey, "A reconfigurable intelligent surface at mmWave based on a binary phase tunable metasurface," *IEEE Open J. Commun. Soc.*, vol. 2, pp. 1055–1064, 2021.

[128] M. Ouyang, Y. Wang, F. Gao, S. Zhang, P. Li, and J. Ren, "Computer vision-aided reconfigurable intelligent surface-based beam tracking: Prototyping and experimental results," 2022, *arXiv:2207.05032*.

[129] Q. Hu, X. Zeng, C. Mao, H. Yang, Q. Wu, J. Tang, X. L. Zhao, and X. Y. Zhang, "Design of a novel 2-bit wideband beam-scanning reconfigurable intelligent surface," in *Proc. IEEE Int. Workshop Electromagn., Appl. Student Innov. Competition (iWEM)*, Nov. 2021, pp. 1–3.

[130] G. C. Trichopoulos, P. Theofanopoulos, B. Kashyap, A. Shekhawat, A. Modi, T. Osman, S. Kumar, A. Sengar, A. Chang, and A. Alkhateeb, "Design and evaluation of reconfigurable intelligent surfaces in real-world environment," *IEEE Open J. Commun. Soc.*, vol. 3, pp. 462–474, 2022.

[131] X. Zeng, Q. Hu, C. Mao, H. Yang, Q. Wu, J. Tang, X. L. Zhao, and X. Yin Zhang, "High-accuracy reconfigurable intelligent surface using independently controllable methods," in *Proc. IEEE Int. Workshop Electromagn., Appl. Student Innov. Competition (iWEM)*, Nov. 2021, pp. 1–3.

[132] M. M. Amri, N. M. Tran, and K. W. Choi, "Reconfigurable intelligent surface-aided wireless communications: Adaptive beamforming and experimental validations," *IEEE Access*, vol. 9, pp. 147442–147457, 2021.

[133] J. Jeong, J. H. Oh, S. Y. Lee, Y. Park, and S.-H. Wi, "An improved path-loss model for reconfigurable-intelligent-surface-aided wireless communications and experimental validation," *IEEE Access*, vol. 10, pp. 98065–98078, 2022.

[134] J. Tang, M. Cui, S. Xu, L. Dai, F. Yang, and M. Li, "Transmissive RIS for 6G communications: Design, prototyping, and experimental demonstrations," 2022, *arXiv:2206.15133*.

[135] K. Li, Y. Naderi, U. Muncuk, and K. R. Chowdhury, "ISurface: Self-powered reconfigurable intelligent surfaces with wireless power transfer," *IEEE Commun. Mag.*, vol. 59, no. 11, pp. 109–115, Nov. 2021.

[136] B. Clerckx, J. Kim, K. W. Choi, and D. I. Kim, "Foundations of wireless information and power transfer: Theory, prototypes, and experiments," *Proc. IEEE*, vol. 110, no. 1, pp. 8–30, Jan. 2022.

[137] N. M. Tran, M. M. Amri, J. H. Park, D. I. Kim, and K. W. Choi, "Multifocus techniques for reconfigurable intelligent surface-aided wireless power transfer: Theory to experiment," *IEEE Internet Things J.*, vol. 9, no. 18, pp. 17157–17171, Sep. 2022.

[138] C. Molero, A. Palomares-Caballero, A. Alex-Amor, I. Parellada-Serrano, F. Gamiz, P. Padilla, and J. F. Valenzuela-Valdes, "Metamaterial-based reconfigurable intelligent surface: 3D meta atoms controlled by graphene structures," *IEEE Commun. Mag.*, vol. 59, no. 6, pp. 42–48, Jun. 2021.

[139] J. Rains, J. U. R. Kazim, L. Zhang, Q. H. Abbasi, M. Imran, and A. Tukmanov, "2.75-bit reflecting unit cell design for reconfigurable intelligent surfaces," in *Proc. IEEE Int. Symp. Antennas Propag. USNC-URSI Radio Sci. Meeting (APS/URSI)*, Dec. 2021, pp. 335–336.

[140] S. Zhao, R. Langwieser, and C. F. Mecklenbraeuker, "Reconfigurable digital metasurface for 3-bit phase encoding," in *Proc. 25th Int. ITG Workshop Smart Antennas*, 2021, pp. 1–6.
[141] J. Rains, J. U. R. Kazim, A. Tukmanov, T. J. Cui, L. Zhang, Q. H. Abbasi, and M. A. Imran, "High-resolution programmable scattering for wireless coverage enhancement: An indoor field trial campaign," *IEEE Trans. Antennas Propag.*, vol. 71, no. 1, pp. 518–530, Jan. 2023.
[142] I. Alamzadeh, G. C. Alexandropoulos, N. Shlezinger, and M. F. Imani, "A reconfigurable intelligent surface with integrated sensing capability," *Sci. Rep.*, vol. 11, no. 1, pp. 1–10, Oct. 2021.
[143] M. Hwang, Y. Youn, S. Chang, D. Kim, C. Lee, D. An, and W. Hong, "Sensor-integrated RIS unit element featuring mutual coupling reduction," in *Proc. IEEE Int. Symp. Radio-Frequency Integr. Technol. (RFIT)*, Aug. 2022, pp. 159–160.
[144] I. Alamzadeh and M. F. Imani, "Sensing and reconfigurable reflection of electromagnetic waves from a metasurface with sparse sensing elements," *IEEE Access*, vol. 10, pp. 105954–105965, 2022.
[145] M. Rossanese, P. Mursia, A. Garcia-Saavedra, V. Sciancalepore, A. Asadi, and X. Costa-Perez, "Designing, building, and characterizing RF switch-based reconfigurable intelligent surfaces," 2022, *arXiv:2207.07121*.
[146] L. Wu, K. Lou, J. Ke, J. Liang, Z. Luo, J. Y. Dai, Q. Cheng, and T. J. Cui, "A wideband amplifying reconfigurable intelligent surface," *IEEE Trans. Antennas Propag.*, vol. 70, no. 11, pp. 10623–10631, Nov. 2022.
[147] R. Matos and N. Pala, "VO_2-based ultra-reconfigurable intelligent reflective surface for 5G applications," *Sci. Rep.*, vol. 12, p. 4497, Mar. 2022.
[148] M. F. Imani, S. Abadal, and P. Del Hougne, "Metasurface-programmable wireless network-on-chip," *Adv. Sci.*, vol. 9, Jun. 2022, Art. no. 2201458.
[149] B. Rana, S.-S. Cho, and I.-P. Hong, "Parameters and measurement techniques of reconfigurable intelligent surfaces," *Micromachines*, vol. 13, no. 11, p. 1841, Oct. 2022.
[150] R. Guirado, G. Perez-Palomino, M. Ferreras, E. Carrasco, and M. Cano-Garcia, "Dynamic modelling of liquid crystalbased metasurfaces and its application to reducing reconfigurability times," *IEEE Trans. Antennas Propag.*, vol. 70, no. 12, pp. 11847–11857, Dec. 2022.
[151] R. Guirado, G. Perez-Palomino, M. Cano-Garcia, M. A. Geday, and E. Carrasco, "Mm-wave metasurface unit cells achieving millisecond response through polymer network liquid crystals," *IEEE Access*, vol. 10, pp. 127928–127938, 2022.
[152] A. Jimenez-Saez, A. Asadi, R. Neuder, D. Wang, and R. Jakoby, "Liquid crystals: The way to scalable and practical reconfigurable intelligent surfaces in 6G," *TechRxiv*, Oct. 2022.
[153] J. Sang, Y. Yuan, W. Tang, Y. Li, X. Li, S. Jin, Q. Cheng, and T. J. Cui, "Coverage enhancement by deploying RIS in 5G commercial mobile networks: Field trials," *IEEE Wireless Commun.*, early access, Dec. 26, 2022, doi: 10.1109/MWC.011.2200356.
[154] K. Liu, Z. Zhang, L. Dai, S. Xu, and F. Yang, "Active reconfigurable intelligent surface: Fully-connected or sub-connected?" *IEEE Commun. Lett.*, vol. 26, no. 1, pp. 167–171, Jan. 2022.

BISWARUP RANA received the Ph.D. degree from the Indian Institute of Engineering Science and Technology, Shibpur, India, in 2017.

He was a Postdoctoral Researcher with the Seoul National University of Science and Technology, South Korea. He is currently with Kongju National University, South Korea. His research interests include the analysis and design of microstrip antennas, substrate-integrated waveguide antennas, phased array antennas, dielectric resonator antennas, implantable antennas, transmitarray, and reconfigurable intelligent surfaces.

SUNG-SIL CHO received the M.S. degree in information and communication engineering from Kongju National University, Cheonan, South Korea, in 2018, where she is currently pursuing the Ph.D. degree. Her research interest includes periodic electromagnetic structures.

IC-PYO HONG (Member, IEEE) received the B.S., M.S., and Ph.D. degrees in electronics engineering from Yonsei University, Seoul, South Korea, in 1994, 1996, and 2000, respectively. From 2000 to 2003, he was with the Information and Communication Division, Samsung Electronics Company, Suwon, South Korea, where he was a Senior Engineer with CDMA Mobile Research. He was a Visiting Scholar with Texas A&M University, College Station, TX, USA, in 2006, and Syracuse University, Syracuse, NY, USA, in 2012. Since 2003, he has been with the Department of Information and Communication Engineering, Kongju National University, Cheonan, South Korea, where he is currently a Professor. His research interests include numerical techniques in electromagnetics and periodic electromagnetic structures.